ADVANCED HEALTHCARE MATERIALS
www.advhealthmat.de

Prototypic Heptamethine Cyanine Incorporating Nanomaterials for Cancer Phototheragnostic

Miguel M. Leitão, Duarte de Melo-Diogo, Cátia G. Alves, Rita Lima-Sousa, and Ilídio J. Correia**

Developing technologies that allow the simultaneous diagnosis and treatment of cancer (theragnostic) has been the quest of numerous interdisciplinary research teams. In this context, nanomaterials incorporating prototypic near infrared (NIR)-light responsive heptamethine cyanines have been showing very promising results for cancer theragnostic. The precisely engineered features of these nanomaterials endow them with the ability to achieve a high tumor accumulation, enabling a tumor's visualization by NIR fluorescence and photoacoustic imaging modalities. Upon interaction with NIR light, the tumor-homed heptamethine cyanine-incorporating nanomaterials can also produce a photothermal/photodynamic effect with a high spatio-temporal resolution and minimal side effects, leading to an improved therapeutic outcome. This progress report analyses the application of nanomaterials incorporating prototypic NIR-light responsive heptamethine cyanines (IR775, IR780, IR783, IR797, IR806, IR808, IR820, IR825, IRDye 800CW, and Cypate) for cancer photothermal therapy, photodynamic therapy, and imaging. Overall, the continuous development of nanomaterials incorporating the prototypic NIR absorbing heptamethine cyanines will cement their phototheragnostic capabilities.

1. Introduction

The development of devices that simultaneously allow the diagnosis and treatment (theragnostic) of cancer has been the focus of different studies performed by worldwide researchers. In this context, light-responsive nanomaterials with theragnostic capabilities have been displaying promising results toward both in vitro and in vivo preclinical cancer models.[1] This therapeutic modality employs nanostructures with well-defined physicochemical properties that confer them with the ability to preferentially accumulate within the tumor.[2] Afterward, the tumor zone is externally irradiated with light and the tumor-homed nanomaterials can absorb it. Upon interaction with light, these nanomaterials can produce a temperature increase (photothermal therapy (PTT)) and/or reactive oxygen species (photodynamic therapy (PDT)), which can cause damage toward cancer cells.[3] The use of near infrared (NIR; 750–1000 nm) light to irradiate these nanomaterials is crucial since this type of radiation has minimal/insignificant interactions with the biological components (e.g., proteins, melanin, water).[4,5] In this way, nanomaterials' mediated phototherapies using NIR light can induce a therapeutic effect with high spatial-temporal resolution and minimal side effects.[5–9]

These nanostructures can also emit fluorescence upon interaction with the NIR light, enabling their use in NIR fluorescence imaging.[7,10] Moreover, the photoinduced heat generated by these nanomaterials can also produce acoustic waves, enabling tissues' visualization through photoacoustic imaging (PAI).[11] This cutting-edge modality allows a higher penetration depth and resolution than fluorescence imaging by taking advantage from the acoustic waves' lower scattering in tissues and the high penetration depth of NIR light.[2,11]

Among the different nanomaterials used for phototheragnostic applications, those formulated by encapsulating NIR responsive small molecules in nanostructures (e.g., micelles, liposomes, porous nanostructures) have been displaying promising results.[2] In this regard, indocyanine green (ICG) loaded nanomaterials have been by far one of the most studied, since this dye is currently approved by the Food and Drug Administration (FDA) for angiography. Moreover, ICG loaded nanomaterials can be used for cancer PTT/PDT[9,12] as well as for imaging.[13] Furthermore, ICG loaded nanostructures are also easier to formulate when compared to the inorganic-based phototheragnostic nanoagents.[14] Nevertheless, ICG has a low photostability and a low fluorescence quantum yield.[2,12] Such has motivated the encapsulation of other heptamethine cyanines (e.g., IR780, IR808, IR825) that exhibit improved optical properties in nanostructures for cancer phototheragnostic.[15]

M. M. Leitão, Dr. D. de Melo-Diogo, C. G. Alves, R. Lima-Sousa, Dr. I. J. Correia
CICS-UBI-Centro de Investigação em Ciências da Saúde
Universidade da Beira Interior
6200-506 Covilhã, Portugal
E-mail: demelodiogo@fcsaude.ubi.pt; icorreia@ubi.pt
Dr. I. J. Correia
CIEPQPF-Departamento de Engenharia Química
Universidade de Coimbra
Rua Sílvio Lima
3030-790 Coimbra, Portugal
The ORCID identification number(s) for the author(s) of this article can be found under https://doi.org/10.1002/adhm.201901665.

DOI: 10.1002/adhm.201901665

In this progress report, the application of nanomaterials incorporating prototypic NIR responsive heptamethine cyanines for cancer PTT, PDT and imaging is analyzed. Initially, the different NIR responsive heptamethine cyanines are reviewed, emphasizing their optical properties and limitations (Section 2). Afterward, the encapsulation of IR780 (Section 3.1), Cypate (Section 3.2), IR808 (Section 3.3), IR820 (Section 3.4), IR825 (Section 3.5), and other heptamethine cyanines (IR775, IR783, IR797, IR806, IRDye 800CW - Section 3.6) in nanomaterials for cancer phototheragnostic is discussed. Finally, an outlook about the state of the art and the future directions are presented (Section 4). For the sake of brevity, the encapsulation of ICG in nanomaterials will not be analyzed since it has been extensively reviewed elsewhere.[16]

2. Heptamethine Cyanines: Properties and Limitations

The FDA-approval of ICG has propelled the use of this NIR absorbing small molecule belonging to the heptamethine cyanine family in cancer theragnostic (reviewed in detail in ref. [2])–**Figure 1**. However, ICG displays critical limitations such as low photostability, rapid blood clearance (within minutes), and inability to specifically target the cancer cells.[12]

To bypass these limitations, researchers have been investigating the potential of other prototypic NIR-absorbing heptamethine cyanines for theragnostic applications. When compared to ICG, some of these NIR dyes have improved optical properties, thus displaying enhanced imaging and therapeutic capabilities (**Table 1**). For instance, IR780 has a higher molar extinction coefficient (265 000–330 000 M^{-1} cm^{-1}, at 780 nm)[17] than ICG (115 000–204 000 M^{-1} cm^{-1}, at 785 nm),[18,19] having an enhanced interaction with NIR light. On the other hand, IR783 has a fluorescence quantum yield of 0.084, which is slightly greater than that of ICG and other heptamethine cyanines (Table 1).[18] The singlet oxygen quantum yield of IR780 and IR808 is also superior to that of ICG, enabling stronger photodynamic effects.[20] Besides these heptamethine cyanines, IR775, IR797, IR806, IR820, IR825, Cypate, IRDye 800CW, and FD-1080 also have promising optical properties (please see Table 1 for further details). In the particular case of IR780, IR783, and IR808, these have been reported to interact with the organic anionic transporter peptides (OATPs), which are overexpressed by cancer cells, enabling their use for tumor imaging[21–24] (please note that imaging applications require the administration of low doses of the imaging agents (e.g., 0.2–0.3 mg kg^{-1}[25,26])).

Despite their potential, in general, these prototypic NIR absorbing heptamethine cyanines have a poor water solubility, affecting their application for cancer PTT/PDT, in which high doses need to be administered for attaining complete tumor ablation.[27] Furthermore, the hydrophobic character of these dyes may promote their aggregation during circulation,[10] leading to undesirable side effects. In fact, the potential toxicity of these dyes is strongly influenced by their hydrophobicity. For instance, IR780 was shown to induce acute toxicity to healthy mice when administered at a dose of 2 mg kg^{-1}.[26] On the other hand, IR808 (which is less hydrophobic due to its carboxylic groups) did not cause appreciable toxicity in normal mice, when administered at a dose of 150 mg kg^{-1}, throughout 7 days.[25] No adverse effects were observed in normal mice that received a 20 mg kg^{-1} dose of IRDye 800CW carboxylate after a 14 days period.[28] Additionally, IR780, IR808, IR820, IR825, and Cypate have been reported to suffer from photodegradation, lowering their potential for continuous tumor monitoring.[29–32]

In general, the limitations of these prototypic heptamethine cyanines can be surpassed by encapsulating/incorporating them in nanomaterials.[21,33] In fact, the loading of these agents in the nanomaterials addresses their solubility concerns.[10,33,34] For instance, Pais-Silva et al. verified that by loading IR780 in poly(ethylene glycol) (PEG)-Vitamin E based micelles, the water solubility of the former increased from 0.4 to 46 μg mL^{-1}.[35] The safety of these NIR heptamethine cyanines is also greatly enhanced through their incorporation into nanomaterials.[26,36–38] For instance, healthy mice injected with PEG-IR780-C_{13} micelles, at an IR780 dose of 7 mg kg^{-1}, did not display toxicity on their major organs nor alterations on the liver- and kidney-function markers after 30 days.[26] The toxicology studies regarding IR825 loaded PEG-poly(maleic anhydride-*alt*-1-octadecene) (PEG-PMAO) micelles (10 mg kg^{-1}) during 40 days did also not reveal any potential adverse

Duarte de Melo-Diogo received his B.Sc. and M.Sc. degrees in biomedical sciences from Universidade da Beira Interior in 2012 and 2014, respectively. In 2018, he concluded his Ph.D. degree in biochemistry from the same university. He is now a researcher at CICS-UBI research center. His research interests are focused on the application of heptamethine cyanine-incorporating nanomaterials and graphene family nanomaterials in cancer phototherapy.

Ilídio J. Correia is an associate professor with habilitation in the Department of Health Sciences at Universidade da Beira Interior. He obtained his B.Sc. and Ph.D. degrees in biochemistry from the University of Lisbon in 1998 and New University of Lisbon in 2003, respectively. His research group is involved in the development of skin and bone substitutes, drug delivery systems, as well as in vitro 3D cell culture models aimed to reproduce solid tumors structural features.

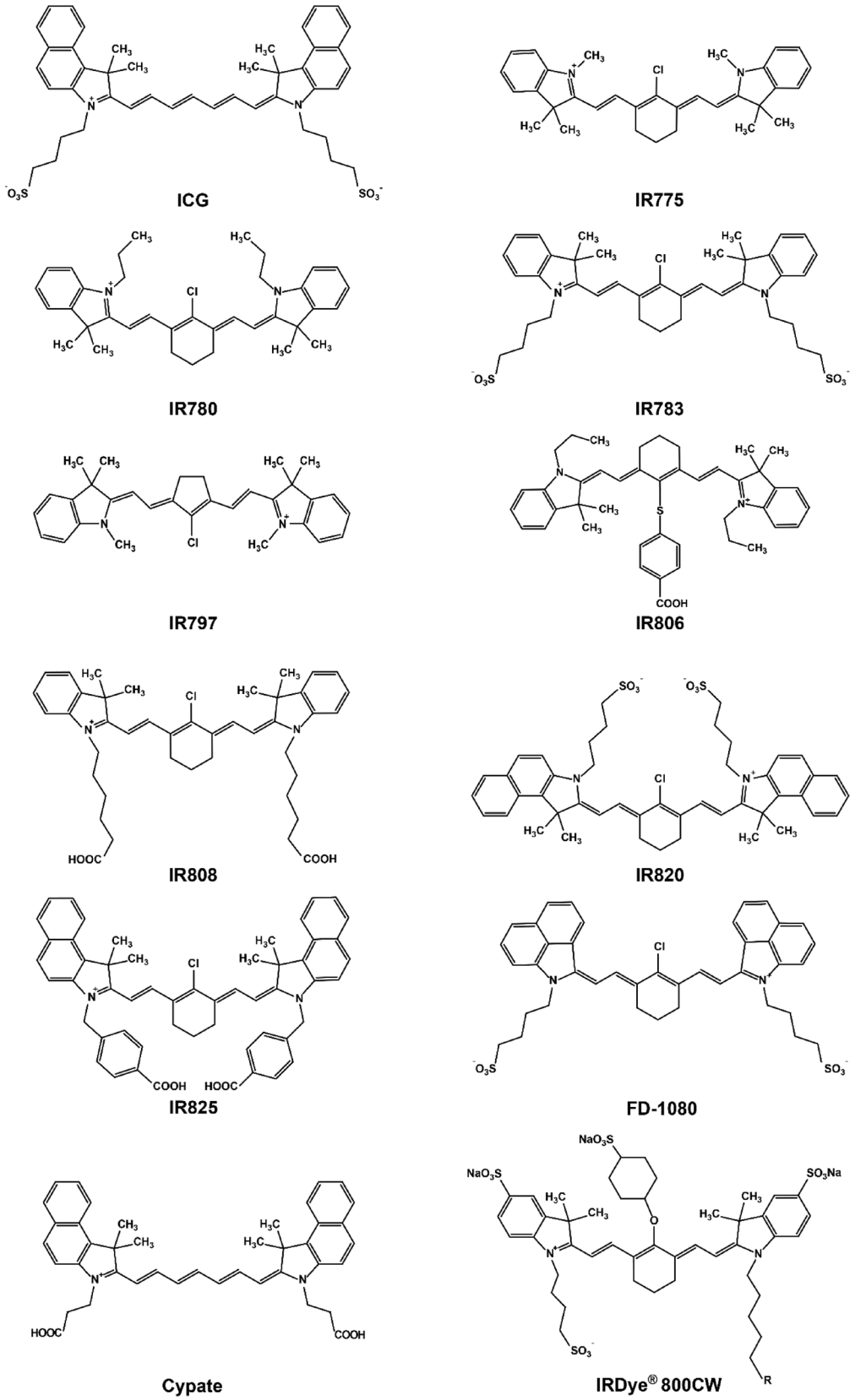

Figure 1. Chemical structure of the prototypic NIR absorbing heptamethine cyanines and of ICG. R: available as IRDye 800CW Carboxylate, NHS ester and maleimide.

Table 1. Photophysical properties of different agents (including NIR agents) used for cancer related applications. Please note that properties vary according to the experimental conditions reported.

Name	λ_{max} [nm]	Molar extinction coefficient [ε; M^{-1} cm^{-1}]	Em_{max} [nm]	Fluorescence quantum yield [Φ_f]	Singlet oxygen quantum yield [Φ_{SO}]	Tumor targeting	Ref.
Cypate	785	216 000	822	0.065	0.02	–	[18]
FD-1080	1012–1044	33 040–73 230	1053–1089	0.18–0.44%	–	–	[75]
ICG	780–785	115 000–204 000	812–822	0.012–0.078	0.008	–	[18,19]
IR775	768	92 300[a)]	790	5.1–5.3%[a)]	–	–	[10,76]
IR780	780	265 000–330 000	798	0.07	0.127	Y	[17,23,77]
IR783	782	261 000	810	0.084	0.007	Y	[18,24]
IR797	792	444.3[b)]	805	5.8%	0.017[c)]	–	[67,76,78]
IR806	806	390[b)]	832[d)]	–	–	–	[68,79]
IR808	776–783	306 000	790–816	5.6–5.9%	0.036	Y	[20,76,80]
IR820	820	202 000	850	0.044	0.02	–	[18]
IR825	825	114 500	–	<0.1%	–	–	[39]
IRDye 800CW	774	240 000–410 000	789	0.034	<0.01	–	[28,81]

[a)]IR775 loaded mPEG-PCL nanoparticles; [b)]value in L g^{-1} cm^{-1}; [c)]IR797 modified with acetylacetone; [d)]approximate value.

effects.[39] Furthermore, the encapsulation of the prototypic heptamethine cyanines in nanostructures can protect them from degradation, leading to an improved photostability.[40,41] For example, Zhang et al. verified that the photothermal capacity of IR825 loaded hollow mesoporous silica nanoparticles is not compromised significantly even after three NIR irradiation cycles.[40] In another study, Xia et al. observed that the photothermal effect mediated by free IR820 decreases drastically after the first cycle of laser irradiation, while IR820 incorporated within porous silicon nanoparticles display almost no loss in their photothermal capacity throughout four irradiation cycles.[41]

As importantly, nanomaterials can present a high tumor-homing capacity arising from their ability to extravasate through the tumor leaky vasculature and to take advantage from the dynamic events occurring in the tumor-associated blood vessels.[42] Once on the tumor microenvironment, nanomaterials must penetrate the tumor mass and become internalized in cancer cells.[5] In this regard, nanomaterials functionalized with targeting ligands can achieve a selective uptake by cancer cells by binding to their overexpressed receptors.[34,37,43,44] The ability of the nanomaterials to benefit from these phenomena is dependent on their physicochemical properties (size, surface charge, corona composition, and presence of targeting ligands), which has been reviewed in detail by our and other research groups elsewhere.[5,45]

For instance, Pan et al. observed that nonencapsulated IR825-NH_2 could not be used for tumor imaging due to its low tumor accumulation.[46] In turn, IR825-polymer conjugate micelles displayed a high tumor uptake, enabling their application for cancer theragnostic.[46] In another work, Song et al. verified that free IR780 and IR780 loaded folic acid (FA)-functionalized PEGylated liposomes present a similar tumor uptake at 1 day post-injection.[47] However, free IR780 was gradually cleared from the tumor zone, emitting minimal fluorescence at the farthest post-injection times. In stark contrast, the IR780 loaded FA-functionalized PEGylated liposomes still remained at the tumor site even after 5 days post-injection. Such enabled continuous tumor monitoring and a photothermal effect that led to tumor eradication.[47]

In this way, heptamethine cyanine incorporating nanomaterials can mediate improved cancer phototheragnostic with minimal off-target toxicity (reviewed in Section 3)–**Figure 2**.

3. Nanomaterials Incorporating Heptamethine Cyanines for Cancer Phototheragnostic

3.1. IR780 Based Nanomaterials

Nanomaterials encapsulating IR780 have been by far one of the most extensively used in cancer PTT[48] and PDT[49] (see **Table 2**). Furthermore, these have also been used for cancer NIR imaging[50] and PAI[49] (see **Table 3**).

Song et al. produced IR780 loaded FA-functionalized PEG-coated liposomes for cancer theragnostic.[47] The optical properties of this formulation enabled the tracking of its biodistribution by NIR fluorescence imaging. Due to the FA functionalization, these liposomes could achieve an up to 2.5-fold and 5-fold higher tumor accumulation than their nontargeted equivalents (PEGylated liposomes) and free IR780, respectively. Owing to their high tumor-homing capacity, the FA-functionalized PEGylated liposomes incorporating IR780 produced a photoinduced heat up to 50 °C, leading to tumor eradication using an ultralow dosage of the formulation (1 mg kg^{-1} of IR780 equivalents). The PTT/PDT capacity of other IR780 based nanomaterials is summarized in Table 2.

Nanoformulations incorporating IR780 and other therapeutic agents can also be prepared for cancer combinatorial phototherapy (Table 2).[51,52] In this regard, Yang et al. prepared PEGylated micelles incorporating IR780 and doxorubicin (DOX) for application in cancer chemo-PTT.[53] These micelles displayed a pH- and thermo-responsiveness, presenting an

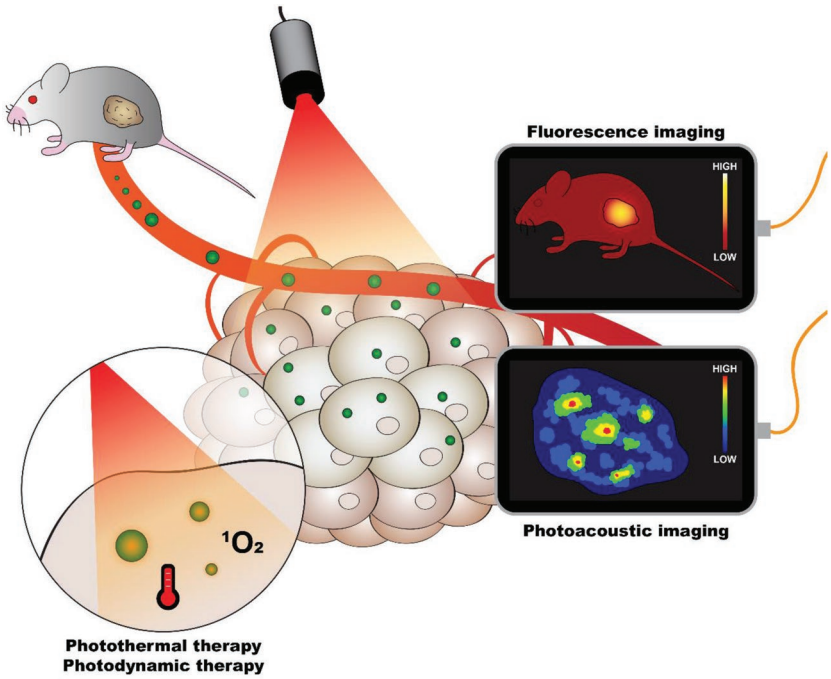

Figure 2. Schematic representation of the phototheragnostic capabilities of the heptamethine cyanine-incorporating nanomaterials.

increased release of the loaded cargo when placed in solutions with an acidic character (i.e., with a pH similar to that exhibited by the tumor microenvironment) and/or upon NIR laser irradiation. In vivo, this formulation had a high tumor-homing capacity, enabling tumor visualization by NIR fluorescence imaging and PAI–**Figure 3** Furthermore, the synergistic chemo-PTT mediated by these micelles led to tumor eradication and inhibition of lung metastasis while the single therapies only led to a reduction of the tumor growth (PTT: IR780 loaded micelles + NIR; chemotherapy: DOX and IR780 loaded micelles).

3.2. Cypate Based Nanomaterials

Cypate incorporating nanomaterials have also been used for cancer PTT/PDT[43] (**Table 4**) as well as for tumor visualization through NIR fluorescence imaging[43] and PAI[54] (Table 3). For this purpose, Cypate (a carboxylated ICG derivative) has been mostly loaded into nanostructures[36,55,56] or conjugated to polymers in order to attain materials capable of assembling into nanostructures.[57,58]

In this context, Miao et al. prepared a PEG-Cypate conjugate that was used in the assembly of micelles for application in cancer PTT/PDT and imaging.[57] In vivo, the PEG-Cypate micelles achieved a higher tumor uptake than free Cypate, enabling a superior tumor visualization through NIR fluorescence imaging. Furthermore, the PTT/PDT effect mediated by the PEG-Cypate micelles induced tumors' eradication while only a reduction of tumors' growth was observed for mice treated with free Cypate plus NIR light. Table 4 summarizes the PTT/PDT capacity of other Cypate based nanomaterials.

Cypate based nanostructures incorporating additional therapeutic agents have also been prepared for application in cancer combinatorial phototherapy (Table 4). In this regard, Jia et al. prepared complexes of Melittin (a cytolytic peptide) and Cypate, which were further coated with hyaluronic acid (HA), for application in cancer chemo-PTT.[36] In vivo, the combined chemo-PTT mediated by the HA coated Melittin/Cypate complex nanoagents induced a potent tumor regression and suppressed the occurrence of lung metastasis. In contrast, mice treated with the single therapies only experienced a reduction in their tumors' growth and displayed metastasis in the lungs (PTT: free Cypate + NIR light; chemotherapy: HA coated Melittin/Cypate complex nanoagents without NIR irradiation).

3.3. IR808 Based Nanomaterials

Nanomaterials incorporating IR808 (also known as MHI-148) have also been showing promising properties for cancer PTT/PDT as well as for the visualization of tumors through NIR fluorescence imaging and PAI[21,30] (**Tables 5** and 3). For this purpose, IR808 (a carboxylated heptamethine cyanine) has been covalently conjugated to polymeric backbones, which are subsequently used in the preparation of IR808 based nanoparticles.[21,30,37]

In this context, Li et al. prepared IR808-HA conjugate nanoparticles, which displayed a higher internalization by cancer cells due to their ability to target the CD44 receptors that are overexpressed by cancer cells.[30] In vivo, the maximum tumor uptake of free IR808 occurred at 12 h post-injection, decreasing rapidly afterward. In contrast, the IR808-HA nanoparticles achieved their highest tumor accumulation at 24 h post-injection and remained at the tumor site for at least 96 h. Due to these facts, the IR808-HA nanoparticles enabled the visualization of the tumors by NIR fluorescence imaging during 96 h (and by PAI for at least 48 h). Furthermore, owing to their high tumor uptake, the PTT mediated by the IR808-HA nanoparticles induced tumor eradication while the PTT mediated by free IR808 only led to a reduction of the tumor growth.

In another work, IR808 was conjugated to the primary amine groups of poly(ethylenimine) (PEI)-PEG-graphene oxide (GO), leading to the assembly of nanostructures with photodynamic potential (conferred by IR808) and enhanced photothermal capacity (conferred by IR808 and GO).[21] The NIR imaging of the tumor bearing mice revealed the ability of these nanomaterials to accumulate at the tumor site. Afterward, the tumor zone was irradiated and the PTT/PDT mediated by the IR808-GO nanomaterials induced complete tumor ablation–**Figure 4**. In contrast, the PTT/PDT mediated by free IR808 only induced a reduction of the tumor growth, which can be explained by its weaker photothermal effect.

Table 2. In vivo therapeutic performance of IR780 based nanostructures.

IR780 based nanostructures	Phototherapy modality	Tumor model	Administration route	Dose[a)]	Laser parameters	Other therapeutic molecules	Therapeutic effect	Ref.
IR780 and DOX loaded liposomes[b)]	PTT	4T1 tumor bearing mice	intratumoral (i.t.)	20 μg	808 nm; 1.0 W cm^{-2}; 5 min	DOX	Tumor eradication	[6]
IR780 and Ce6[c)] loaded HSA[d)] nanoparticles	PTT/PDT	CT-26 tumor bearing mice	intravenous (i.v.)	0.4 mg kg^{-1} of Ce6	660 nm; 0.04 W cm^{-2}; 15 min 808 nm; 0.533 W cm^{-2}; 40 s	Ce6	Tumor eradication	[82]
IR780 loaded FA functionalized PEGylated liposomes[e)]	PTT	SKOV-3 tumor bearing mice	i.v.	1 mg kg^{-1}	808 nm; 1.0 W cm^{-2}; 10 min	–	Tumor eradication	[47]
IR780 loaded HA functionalized micelles[f)]	PTT/PDT	MDA-MB-231 tumor bearing mice	i.v.	1.4 mg kg^{-1}	808 nm; 0.8 W cm^{-2}; 10 min	–	Tumor eradication	[83]
IR780 and DOX loaded PEGylated micelles[g)]	PTT	4T1 tumor bearing mice	i.v.	0.5 mg kg^{-1} (3 times)	808 nm; 1.0 W cm^{-2}; 5 min (3 times)	DOX	Tumor eradication	[53]
IR780 loaded FA-Graphene quantum dots	PTT	HeLa tumor bearing mice	i.v.	2 mg kg^{-1} of nanostructures	808 nm; 1.0 W cm^{-2}; 5 min	–	Tumor eradication	[84]
RBC[h)] membrane-coated IR780 and DTX[i)] loaded PCL-PEG-PCL nanoparticles	PTT/PDT	MCF-7 tumor bearing mice	i.v.	1.67 mg kg^{-1} (3 times)	808 nm; 1.5 W cm^{-2}; 5 min	DTX	Tumor eradication	[49]
IR780 and AMD3100 loaded liposomes[j)]	PTT	4T1/Luc tumor bearing mice	i.v.	1.4 mg kg^{-1} (8 times)	808 nm; 1.0 W cm^{-2}; 4 min	AMD3100	Tumor eradication	[85]
IR780 loaded CXCR4-targeted liposomes[k)]	PTT	4T1/Luc tumor bearing mice	i.v.	1.4 mg kg^{-1} (8 times)	808 nm; 1.0 W cm^{-2}; 5 min	AMD3100	Tumor eradication	[86]
IR780 loaded FA functionalized PEGylated liposomes[l)]	PTT	U87 tumor bearing mice	i.v.	10 μg	808 nm; 1.0 W cm^{-2}; 2 min	–	Tumor regression	[87]
IR780 and DOX loaded PEGylated micelles[m)]	PTT	MCF-7/DOX tumor bearing mice	i.v.	20 μg (twice)	808 nm; 4.0 W cm^{-2}; 5 min (twice)	DOX	Tumor regression	[88]
RV[n)] loaded IR780-BSA[o)]-TiS_2 nanosheets	PTT	CT-26 tumor bearing mice	i.v.	0.5 mg kg^{-1}	808 nm; 0.3 W cm^{-2}; 3 min	RV TiS_2	Tumor regression	[48]
IR780 loaded iRGD[p)]-functionalized Dextran-poly(lysine)-based nanostructures incorporating fluorocarbons	PDT	4T1 tumor bearing mice	i.v.	0.5 mg kg^{-1}	808 nm; 2.0 W cm^{-2}; 5 min	Fluorocarbons	Tumor regression	[89]
IR780 and SPION[q)] loaded PEGylated HSA nanoparticles	PTT	CT-26 tumor bearing mice	i.v.	1 mg kg^{-1}	808 nm; 1.0 W cm^{-2}; 5 min	SPION	Tumor regression	[90]
IR780 and Ce6 loaded TPP-functionalized PEGylated liposomes[r)]	PTT/PDT	HeLa tumor bearing mice	i.v.	1.5 mg kg^{-1} (twice)	660 nm; 0.5 W cm^{-2}; 5 min 808 nm; 1.0 W cm^{-2}; 5 min (twice)	Ce6	Tumor regression	[51]
IR780 and DTX loaded HSA nanoparticles	PTT/PDT	22RV1 tumor bearing mice	i.v.	5 mg kg^{-1}	808 nm; 1.0 W cm^{-2}; 4 min	DTX	Tumor regression	[91]
IR780 and DOX loaded PEGylated liposomes[s)]	PTT	KB tumor bearing mice	i.v.	10 mg kg^{-1} of DOX	780 nm; 1.0 W cm^{-2}; 15 min	DOX	Tumor regression	[92]
IR780 and DOX loaded PDA[t)]-coated TPGS[u)]- micelles	PTT/PDT	MCF-7/ADR tumor bearing mice	i.v.	3 mg kg^{-1} of DOX (10 times)	808 nm; 0.5 W cm^{-1}; 5 min (20 times)	PDA DOX	Tumor regression	[93]
PEG-IR780-C_{13} micelles	PTT	RENCA tumor bearing mice	i.v.	40 mg kg^{-1} of nanostructures	808 nm; 0.8 W cm^{-2}; 10 min	–	Tumor regression	[94]

Table 2. Continued.

IR780 based nanostructures	Phototherapy modality	Tumor model	Administration route	Dose[a)]	Laser parameters	Other therapeutic molecules	Therapeutic effect	Ref.
IR780 and Perfluoropentane loaded cRGD-functionalized PEGylated nanoparticles[v)]	PTT	B16 tumor bearing mice	i.v.	1 mg of nanostructures	808 nm; 2.0 W cm^{-2}; 5 min	Perfluoropentane	Tumor growth inhibition	[38]
IR780 and Cabazitaxel loaded PEGylated micelles[w)]	PTT	4T1 tumor bearing mice	i.v.	5 mg kg^{-1}	808 nm; 0.5 W cm^{-2}; 5 min	Cabazitaxel	Tumor growth inhibition	[95]
CPT[x)]-*ss*-CPT and Lactobionic acid-IR780 mixed nanoparticles	PTT	Hep1-6 tumor bearing mice	i.v.	5.74 µmol kg^{-1} of nanostructures	660 nm; 1.0 W cm^{-2}; 5 min	CPT	Tumor growth inhibition	[96]
IR780 loaded transferrin nanoparticles	PTT/PDT	CT-26 tumor bearing mice	i.v.	20 mg kg^{-1}	808 nm; 1.0 W cm^{-2}; 5 min	–	Tumor growth inhibition	[97]
IR780 and PFOB[y)] loaded cRGDK functionalized PEG-PCL micelles	PDT	MDA-MB-231 tumor bearing mice	i.v.	20 µg	808 nm; 2.0 W cm^{-2}; 20 s	PFOB	Tumor growth reduction	[98]
IR780 and PFOB loaded PEG-PLGA nanoparticles	PTT/PDT	A549 tumor bearing mice	i.t.	20 µg	808 nm; 2.0 W cm^{-2}; 1 min	PFOB	Tumor growth reduction	[99]
IR780 and PTX[z)] loaded isopentyl nitrite-HSA nanoparticles	PTT/PDT	4T1 tumor bearing mice	i.v.	40 µg	808 nm; 0.8 W cm^{-2}; 45 s (twice)	PTX Nitric oxide	Tumor growth reduction	[100]
IR780 loaded PEGylated micelles[aa)]	PTT	MCF-7 tumor bearing mice	i.v.	4 mg kg^{-1}	808 nm; 1.6 W cm^{-2}; 5 min	–	Tumor growth reduction	[101]
DOX loaded IR780-micelles[ab)]	PTT/PDT	MCF-7 tumor bearing mice	i.v.	0.5 mg kg^{-1} (10 times)	808 nm; 0.5 W cm^{-2}; 3 min (10 times)	DOX	Tumor growth reduction	[102]
DOX loaded PEG-IR780-C_{13}-based liposomes[ac)]	PTT	CT-26 tumor bearing mice	i.v.	6.2 mg kg^{-1} of PEG-IR780-C_{13}	808 nm; 1.0 W cm^{-2}; 3 min	DOX	Tumor growth reduction	[103]
Sunitinib and IR780 loaded liposomes[ad)]	PTT	4T1 tumor bearing mice	i.v.	1 mg kg^{-1} (8 times)	808 nm; 1.0 W cm^{-2}; 4 min (8 times)	Sunitinib	Tumor growth reduction	[52]
IR780 loaded lipid nanocarriers[ae)]	PTT	CT-26 tumor bearing mice	via oral gavage	6.5 mg kg^{-1} (twice)	808 nm; 2.0 W cm^{-2}; 1 min	–	Tumor growth reduction	[104]
IR780 loaded Hb[af)] nanoparticles	PTT	CT-26 tumor bearing mice	via oral gavage	6.5 mg kg^{-1} (twice)	808 nm; 2.0 W cm^{-2}; 1 min (twice)	–	Tumor growth reduction	[105]
IR780 loaded PEGylated liposomes[ag)]	PTT	4T1/Luc tumor bearing mice	i.v.	25 mg kg^{-1} of nanostructures	808 nm; 1.0 W cm^{-2}; 10 min	–	Tumor growth reduction	[106]

[a)]Dose of heptamethine cyanine (unless stated otherwise); [b)]formulated using 1,2-dipalmitoyl-*sn*-glycero-3-phospholcholine (DPPC), 1-myristoyl-2-palmitoyl-*sn*-glycero-3-phosphocholine, and 1,2-distearoyl-*sn*-glycero-3-phosphoethanolamine-*N*-[methoxy(polyethylene glycol)] (DSPE-PEG); [c)]chlorin e6; [d)]human serum albumin; [e)]formulated with DPPC, cholesterol, DSPE-PEG-Folate; [f)]formulated with an HA-cholesterol conjugate; [g)]formulated using PEG-poly(acrylamide-*co*-acrylonitrile-*co*-vinylimidazole); [h)]red blood cells; [i)]docetaxel; [j)]prepared using soybean phospholipids, trilaurin, cholesterol and sodium dodecyl sulfate; [k)]formulated with phosphatidylcholine, medium chain triglycerides, trilaurin and AMD3100; [l)]formulated with DPPC, DSPE-PEG-FA; [m)]formulated with PEG-poly(*N*-acryloylglycinamide-*co*-acrylonitrile); [n)]resveratrol; [o)]bovine serum albumin; [p)]tripeptide arginine-glycine-aspartic-acid; [q)]superparamagnetic iron oxide nanoparticles; [r)]formulated with DPPC, Cholesterol, DSPE-PEG and DSPE-PEG-Triphenylphosphonium (TPP); [s)]formulated with DPPC, cholesterol, DSPE-PEG and DSPE-PEG-FA; [t)]polydopamine; [u)]d-α-tocopheryl poly(ethylene glycol) 1000 succinate; [v)]cyclic RGD (cRGD) functionalized PLGA-PEG-based nanoparticles; [w)]formulated with PEG-*b*-poly(acrylamide-*co*-acrylonitrile); [x)]camptothecin; [y)]perfluorooctyl bromide; [z)]paclitaxel; [aa)]prepared using poly(2-hydroxyethyl methacrylate)-*g*-(poly(acrylic acid) (PAA)-PEG); [ab)]formulated using an IR780-chitosan-stearic acid conjugate; [ac)]formulated using lecithin, cholesterol and PEG-IR780-C_{13} conjugate; [ad)]formulated using soybean phospholipids; [ae)]soy lecithin, trilaurin and Labrafac CC; [af)]hemoglobin; [ag)]formulated with DPPC, cholesterol and DSPE-PEG.

3.4. IR820 Based Nanomaterials

The application of nanoparticles incorporating IR820 in cancer PTT/PDT and NIR imaging and PAI has also been extensively investigated (**Tables 6** and 3).[59–61] For instance, Huang et al. incorporated IR820 in ferritin nanocages, demonstrating the ability of these nanostructures to accumulate at the tumor and image it through PAI.[60] Upon NIR laser irradiation, these nanostructures induced a temperature increase of about 24 °C, leading to complete tumor eradication.

Table 3. Application of heptamethine cyanine based nanostructures for in vivo NIR tumor imaging.

Heptamethine cyanine based nanostructures	Tumor model	Administration route	Dose[a)]	PAI	NIR fluorescence imaging	Ref.
IR780 and DOX loaded liposomes[c)]	4T1 tumor bearing mice	i.t.	non disclosed (N.D.)	–	Y	[6]
IR780 and DOX loaded PEGylated liposomes[d)]	KB tumor bearing mice	i.v.	N.D.	–	Y	[92]
IR780 loaded FA functionalized PEGylated liposomes	U87 tumor bearing mice	i.v.	N.D.	–	Y	[87]
IR780 loaded V7-fuctionalized chitosan coated mesoporous silica nanoparticles	ES-2 or A2780 tumor bearing mice	i.v.	0.05 nmol	Y	–	[107]
IR780 loaded PEGylated liposomes[e)]	U87M2/Luc tumor bearing mice	i.v.	2 nmol	–	Y	[108]
IR780 and PFOB loaded cRGDK functionalized PEG-PCL micelles	MDA-MB-231 tumor bearing mice	i.v.	20 μg	Y	Y	[98]
IR780 loaded Pluronic F-127 nanoparticles	SKBR3 tumor bearing mice	i.v.	20 μg of nanostructures	–	Y	[50]
IR780 loaded HSA-based nanoparticles	BxPC-3 tumor bearing mice	i.v.	22.5 μg	–	Y	[109]
IR780 and DOX loaded PEGylated micelles	MCF-7/DOX tumor bearing mice	i.v.	20 μg (twice)	–	Y	[88]
IR780 and Cabazitaxel loaded PEGylated micelles	4T1 tumor bearing mice	i.v.	100 μg	–	Y	[95]
IR780 and Perfluoropentane loaded cRGD-functionalized PEGylated nanoparticles	B16 tumor bearing mice	i.v.	1 mg of nanostructures	Y	Y	[38]
CPT-*ss*-CPT and Lactobionic acid-IR780 mixed nanoparticles	Hep1-6 tumor bearing mice	i.v.	1.5 μmol kg^{-1}	–	Y	[96]
IR780 and AMD3100 loaded liposomes[f)]	4T1/Luc tumor bearing mice	i.v.	0.3 mg kg^{-1}	–	Y	[85]
IR780 and DOX loaded PEGylated micelles[g)]	4T1 tumor bearing mice	i.v.	0.3 mg kg^{-1}	Y	Y	[53]
IR780 and SPION loaded PEGylated HSA nanoparticles	CT-26 tumor bearing mice	i.v.	0.3 mg kg^{-1}	–	Y	[90]
IR780 and Sunitinib loaded liposomes[h)]	4T1 tumor bearing mice	i.v.	0.3 mg kg^{-1}	–	Y	[52]
IR780 loaded CXCR4-targeted liposomes[i)]	4T1-luc tumor bearing mice	i.v.	0.3 mg kg^{-1}	–	Y	[86]
IR780 loaded CXCR4-targeted liposomes[j)]	HSC-T6 tumor bearing mice	i.v.	0.3 mg kg^{-1}	–	Y	[110]
IR780 loaded transferrin nanoparticles	CT-26 tumor bearing mice	i.v.	0.3 mg kg^{-1}	–	Y	[97]
DOX loaded IR780-micelles	MCF-7, H22 and 4T1 tumor bearing mice	i.v.	0.5 mg kg^{-1}	–	Y	[102]
IR780 and Ce6 loaded TPP-functionalized PEGylated liposomes[k)]	HeLa tumor bearing mice	i.v.	0.5 mg kg^{-1}	Y	Y	[51]
IR780 loaded iRGD-functionalized Dextran-poly(lysine)-based nanostructures incorporating fluorocarbons	4T1 tumor bearing mice	i.v.	0.5 mg kg^{-1}	Y	Y	[89]
IR780 and Ce6 loaded HSA nanoparticles	CT-26 tumor bearing mice	i.v.	0.7 mg kg^{-1}	–	Y	[82]
IR780 loaded HA functionalized micelles	MDA-MB-231 tumor bearing mice	i.v.	0.7 mg kg^{-1}	Y	Y	[83]
DOX loaded PEG-IR780-C_{13}-based liposomes[l)]	CT-26 tumor bearing mice	i.v.	0.75 mg kg^{-1} of PEG-IR780-C_{13}	–	Y	[103]
IR780 loaded FA functionalized PEGylated liposomes	SKOV-3 tumor bearing mice	i.v.	1 mg kg^{-1}	–	Y	[47]
IR780 loaded Hb nanoparticles	CT-26 tumor bearing mice	via oral gavage	1 mg kg^{-1}	–	Y	[105]
IR780 loaded lipid nanocarriers[m)]	CT-26 tumor bearing mice	via oral gavage	1 mg kg^{-1}	–	Y	[104]
IR780 loaded PEGylated micelles[n)]	MCF-7 tumor bearing mice	i.v.	1 mg kg^{-1}	–	Y	[101]
PEG-IR780-C_{13} micelles	RENCA tumor bearing mice	i.v.	1 mg kg^{-1} of nanostructures	–	Y	[94]
IR780 loaded PEGylated liposomes	4T1/Luc tumor bearing mice	i.v.	1.1 mg kg^{-1}	Y	Y	[106]
IR780 and PTX loaded isopentyl nitrite-HSA nanoparticles	4T1 tumor bearing mice	i.v.	1.5 mg kg^{-1}	–	Y	[100]
RBC membrane-coated IR780 and DTX loaded PCL-PEG-PCL nanoparticles	MCF-7 tumor bearing mice	i.v.	1.6 mg kg^{-1}	Y	Y	[49]

Table 3. Continued.

Heptamethine cyanine based nanostructures	Tumor model	Administration route	Dose[a)]	PAI	NIR fluorescence imaging	Ref.
IR780 loaded FA-Graphene quantum dots	HeLa tumor bearing mice	i.v.	2 mg kg^{-1} of nanostructures	–	Y	[84]
IR780 and DOX loaded PDA-coated TPGS- micelles	MCF-7/ADR tumor bearing mice	i.v.	3 mg kg^{-1} of nanostructures	–	Y	[93]
IR780 and DTX loaded HSA nanoparticles	22RV1 tumor bearing mice	i.v.	3 mg kg^{-1}	–	Y	[91]
Cypate incorporating PEGylated nanoparticles[o)]	HeLa tumor bearing mice	i.v.	23 µg	–	Y	[111]
PEG-Cypate micelles	B16F10 tumor bearing mice	i.v.	0.25 mg kg^{-1}	–	Y	[57]
Cypate loaded Folate-functionalized PEGylated based micelles	MDA-MB-231 tumor bearing mice	i.v.	1 mg kg^{-1} of nanostructures	–	Y	[44]
Cypate-BSA based nanoparticles	4T1 tumor bearing mice	i.v.	1.5 mg kg^{-1}	Y	Y	[54]
Cypate loaded HA based nanoparticles	MCF-7 tumor bearing mice	i.v.	2 mg kg^{-1}	–	Y	[43]
HA coated Melittin/Cypate nanoagents	4T1 tumor bearing mice	i.v.	3 mg kg^{-1}	–	Y	[36]
Cypate and DPAE loaded PEGylated micelles[p)]	4T1 tumor bearing mice	i.v.	7.5 mg kg^{-1}	–	Y	[112]
Cypate and Pt(IV) prodrug loaded PEGylated micelles[q)]	A549R tumor bearing mice	i.v.	7.5 mg kg^{-1}	–	Y	[55]
Cypate and PTX loaded PEGylated nanorparticles[r)]	4T1 tumor bearing mice	i.v.	7.5 mg kg^{-1}	–	Y	[56]
Cypate and 17AAG loaded PEGylated micelles[s)]	A549 tumor bearing mice	i.v.	7.5 mg kg^{-1}	–	Y	[113]
Cypate-PEG-GO	4T1 tumor bearing mice	i.v.	7.5 mg kg^{-1}	–	Y	[114]
Cypate and Ce6 loaded PEGylated micelles[q)]	4T1 tumor bearing mice	i.v.	7.5 mg kg^{-1}	Y	Y	[115]
DOX loaded PEGylated cypate- mesoporous silica nanoparticles	4T1 tumor bearing mice	i.v.	8.5 mg kg^{-1}	–	Y	[116]
Cypate loaded PEGylated micelles[q)]	A549 tumor bearing mice	i.v.	10 mg kg^{-1}	–	Y	[117]
IR808-HA nanoparticles	A549 tumor bearing mice	i.v.	10 µg	Y	Y	[30]
IR808-PEG-PSMA coated MnO nanoparticles	MCF-7 tumor bearing mice	i.v.	50 µg	Y	Y	[37]
IR808-mesoporous silica shell coated Gd silicate nanoparticles	LLC/LL2 tumor bearing mice	i.v.	0.25 µmol kg^{-1}	–	Y	[118]
PTX loaded IR808-HGC micelles	4T1 and SCC7 tumor bearing mice	i.v.	0.12 mg kg^{-1}	–	Y	[119]
IR808-PEG-DSPE coated SPIONs	SCC7 tumor bearing mice	i.v.	0.2 mg kg^{-1}	–	Y	[120]
IR808-PEI-PEG-GO	A549 and Lewis tumor bearing mice	i.v.	0.5 mg kg^{-1} of nanostructures	–	Y	[21]
IR820-poly(histidine)-DPPE[t)] nanoparticles	MCF-7 tumor bearing mice	i.v.	N.D.	–	Y	[121]
PEGylated IR820-micelles[u)]	BxPC-3 tumor bearing mice	i.v.	15 µg of IR820-COOH	–	Y	[122]
IR820 loaded ferritin nanocages	4T1 tumor bearing mice	i.v.	400 µg	Y	–	[60]
IR820-PTX nanoparticles	4T1 tumor bearing mice	i.v.	4.2 mg kg^{-1} of nanostructures	–	Y	[61]
PEGylated IR820-conjugated poly(β-amine ester) and ZnPP-poly(β-amine ester) micelles	A549 tumor bearing mice	i.v.	5 mg kg^{-1} of nanostructures	Y	–	[7]
IR825 and CA4 loaded siHSP70/PEI-PLA micelles	MDA-MB-231 tumor bearing mice	i.v.	N.D.	Y	–	[123]
IR825 and DOX loaded PEG-PAA-PEI aggregates	4T1 tumor bearing mice	i.v.	N.D.	Y	–	[124]
IR825 loaded TCPP crosslinked PEGylated micelles	4T1 tumor bearing mice	i.v.	100 µg	Y	–	[33]
PFOB loaded HA-IR825 nanoparticles	HT-29 tumor bearing mice	i.v.	500 µg of nanostructures	Y	–	[125]
dc-IR825 and 17AAG loaded HSA nanoparticles	4T1 tumor bearing mice	i.v.	1 mg kg^{-1}	–	Y	[64]
IR825 and DOX loaded perylene diimide-based nanoplatforms	U87MG tumor bearing mice	i.v.	1 mg of nanostructures	Y	–	[126]
dc-IR825 loaded TPGS micelles	U14 tumor bearing mice	i.v.	3 mg kg^{-1}	Y	Y	[65]
PEG-IR825 and HA-PDA anchored rGO	MDA-MB-231 tumor bearing mice	i.v.	5 mg kg^{-1} of nanostructures	–	Y	[127]

Table 3. Continued.

Heptamethine cyanine based nanostructures	Tumor model	Administration route	Dose[a)]	PAI	NIR fluorescence imaging	Ref.
mPEG-*b*-poly(L-aspartic acid sodium salt)-IR825[b)] conjugate micelles	U14 tumor bearing mice	i.v.	10 mg kg^{-1} of nanostructures	–	Y	[46]
me-IR825 loaded Pluronic F-127 based nanoparticles	U14 tumor bearing mice	i.v.	300 mg kg^{-1} of nanostructures	Y	Y	[66]
IR775 loaded HSA-based nanoparticles	4T1 tumor bearing mice	i.v.	N.D.	–	Y	[128]
IR775 loaded HSA-based nanoparticles	CT-26 tumor bearing mice	i.v.	N.D.	–	Y	[129]
IR783 conjugated with cRGD-PEG-dendritic poly(lysine)	U87 tumor bearing mice	i.v.	15 nmol	–	Y	[70]
IR797 loaded PEG-PMAO micelles	HeLa tumor bearing mice	i.v.	42 nmol	Y	Y	[67]
IR775 loaded PEG-Hb nanoparticles	H22 tumor bearing mice	i.v.	0.3 mg kg^{-1}	–	Y	[130]
IR775 loaded mPEG-PCL nanoparticles	A2780/CDDP tumor bearing mice	i.v.	0.75 mg kg^{-1}	–	Y	[10]
IR783-PEG-DSPE and CREKA[v)]-PEG-DSPE coated oxidized MWNTs[w)]	A549 tumor bearing mice	i.v.	4 mg kg^{-1} of nanostructures	–	Y	[69]
IRDye 800CW labeled PEGylated liposomes[x)]	BLM tumor bearing mice	i.v.	1 µmol of nanostructures	–	Y	[71]
IRDye 800CW labeled PSMA-targeted PEGylated starch coated Fe_3O_4 nanoparticles	PC3 tumor bearing mice	i.v.	250 µg of nanostructures	–	Y	[72]
GX1 peptide-IRDye 800CW-PVA/PLA nanoparticles	U87MG tumor bearing mice	i.v.	1 mg	–	Y	[131]
IRDye 800CW labeled HA-PEG coated hollow Prussian blue nanoparticles[y)]	HeLa tumor bearing mice	i.v.	10 mg kg^{-1} of nanostructures	–	Y	[132]

[a)]Dose of heptamethine cyanine (unless stated otherwise); [b)]IR825 derivative modified with a primary amine; [c)]formulated using DPPC, 1-myristoyl-2-palmitoyl-*sn*-glycero-3-phosphocholine, and DSPE-PEG; [d)]formulated with DPPC, cholesterol, DSPE-PEG and DSPE-PEG-FA; [e)]formulated with distearoylphosphatidylcholine (DSPC), cholesterol and DSPE-PEG; [f)]prepared using soybean phospholipids, trilaurin, cholesterol and sodium dodecyl sulfate; [g)]formulated using PEG-poly(acrylamide-*co*-acrylonitrile-*co*-vinylimidazole); [h)]formulated using soybean phospholipids; [i)]formulated with phosphatidylcholine, medium-chain triglycerides, trilaurin and AMD3100; [j)]formulated with egg phosphatidylcholine, cholesterol and AMD3100; [k)]formulated with DPPC, cholesterol, DSPE-PEG and DSPE-PEG-TPP; [l)]formulated using lecithin, cholesterol and PEG-IR780-C_{13} conjugate; [m)]formulated with soy lecithin, trilaurin, and Labrafac CC; [n)]prepared using poly(2-hydroxyethyl methacrylate)-*g*-(PAA-PEG); [o)]formulated with PEG-bilirubin and biotin-PEG-bilirubin; [p)]formulated with PEG-PCL-poly((2-(piperidin-1-yl) ethyl methacrylate); [q)]formulated with mPEG-poly (L-aspartic acid(decylamine)) (mPEG-PAsp(DA)); [r)]formulated with PEG-PCL-SS-P(*N*-isopropylacrylamide-*co*-*N*,*N*-dimethylacrylamide) (PEG-PCL-SS-P(NIPAM-*co*-DMA)); [s)]formulated with PEG-PCL; [t)]1,2-dipalmitoyl-*sn*-glycero-3-phosphoethanolamine; [u)]formulated using PEG-polylactide (PLA)-*co*-poly(5-methyl-5-allyloxycarbonyl-1,3-dioxan-2-one)-*g*-(IR820-*co*-Gemcitabine)); [v)]Cys-Arg-Glu-Lys-Ala peptide; [w)]multiwalled carbon nanotubes; [x)]formulated with DPPC, DSPC, DSPE-PEG and 3-(2-pyridyl)-dithiopropionyl-PEG-DSPE; [y)]formulated by conjugating HA-*g*-PEG to PAH/PAA coated hollow prussian blue nanoparticles.

In another work, Valcourt et al. demonstrated that the PTT mediated by poly(lactic-*co*-glycolic acid) (PLGA) nanoparticles loaded with IR820 could induce tumors regression.[62] Still, in order to achieve such effect, 4 different nanomaterials' administration and irradiation sessions were required.

In this way, IR820 based nanomaterials have also been combined with other therapeutic agents with the intent to improve their therapeutic efficacy (Table 6). In this regard, Li et al. improved the efficacy of IR820 loaded Lyp-1 modified micelles by incorporating docetaxel in the nanoformulation.[63] In vivo, the combinatorial chemo-PTT/PDT mediated by these micelles induced tumor eradication using a relatively low dose of the photo-responsive agent (2 mg kg^{-1} of IR820).

3.5. IR825 Based Nanomaterials

The loading of IR825 into different nanostructures for application in cancer PTT/PDT and imaging (NIR fluorescence imaging and PAI) has also been described in several reports[27,33,46]—see details in **Tables 7** and 3. Alternatively, Pan et al. prepared an IR825-derivative modified with a primary amine in order to conjugate it to mPEG-poly(L-aspartic acid sodium salt), rendering an amphiphilic copolymer capable of self-assembling into micelles.[46] In vivo, the IR825-micelles displayed a long blood circulation time, achieving a high tumor accumulation that allowed tumors' NIR imaging over time. Furthermore, the PTT mediated by the IR825-micelles induced tumors eradication while the combination of primary amine modified-IR825 with NIR light did not produce a therapeutic effect due to the low tumor uptake of the free dye. Furthermore, the Wu group also prepared other IR825 derivatives termed as dc-IR825[64,65] and me-IR825,[66] and whose encapsulation in nanomaterials enabled an effective PTT/PDT in vivo.

Furthermore, combinatorial cancer phototherapies based on IR825-incorporating nanomaterials have also been developed by including additional agents in the nanomaterials (Table 7). For instance, Liu et al. produced PEGylated polymeric micelles loaded with IR825 and cross-linked with 5,10,15,20-tetrakis(4-carboxyphenyl) porphyrin (TCPP, a porphyrin derivative that is also a 660 nm absorbing photodynamic agent) for application in cancer PTT/PDT.[33] These micelles were able to reach the tumor tissue, enabling its visualization by PAI. Subsequently, the irradiation of the tumor zone with NIR and 660 nm lights

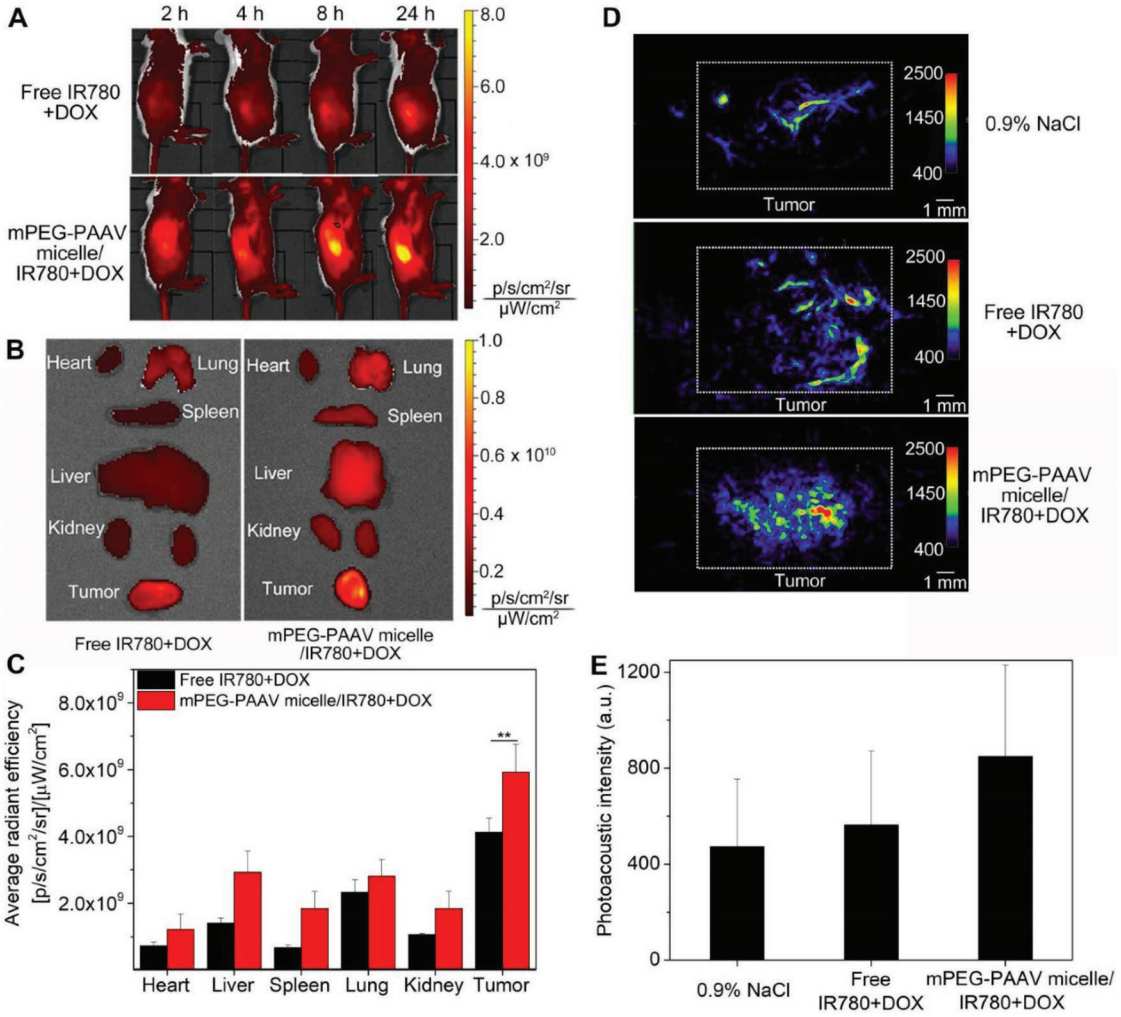

Figure 3. Imaging capabilities of the PEGylated micelles incorporating IR780 and DOX. A) NIR fluorescence imaging of mice treated with different formulations. B) Ex vivo NIR fluorescence imaging and C) quantitative IR780 tumor uptake. D) PAI of the tumors and E) photoacoustic intensity at the tumor site after the different treatments. mPEG-PAAV micelles/IR780+DOX: PEGylated micelles incorporating IR780 and DOX. Reproduced with permission.[53] Copyright 2018, Ivyspring International Publishers.

produced a photothermal-photodynamic effect that reduced tumors' growth. In contrast, a weaker therapeutic effect was observed on mice solely irradiated with NIR light (PTT) and 660 nm light (PDT).

3.6. Other Heptamethine Cyanine Based Nanomaterials

Nanomaterials incorporating IR775, IR797, and IR806 have not yet been as widely explored for cancer theragnostic as those described above (**Tables 8** and 3).[10,67,68] Nevertheless, these have demonstrated promising results which should motivate further investigation on their applicability for cancer PTT/PDT and imaging (Tables 8 and 3).

For instance, Duong et al. demonstrated that PEG-poly(caprolactone) (PCL) nanoparticles loaded with IR775 or IR797 possess optical properties that may enable their use for cancer NIR imaging and PTT/PDT.[10] In another work, Deng et al. prepared IR806 (a carboxylated IR780 derivative obtained by reacting IR780 with 4-mercaptobenzoic acid) and conjugated it to primary amine-capped PEGylated $MnFe_2O_4$ nanoparticles.[68] This system displayed photodynamic (derived from IR806) and enhanced photothermal (arising from IR806 and $MnFe_2O_4$) capabilities, thus mediating an improved PTT/PDT in vivo.[68]

The labeling of other nanomaterials with IR783[69,70] and IRDye 800CW[71,72] (Table 3) also enabled the analysis of nanomaterials' biodistribution and the visualization of the tumoral mass overtime.

4. Conclusion and Outlook

In this progress report, the recent advances regarding the use of nanomaterials incorporating prototypic NIR heptamethine cyanines for cancer phototheragnostic were analyzed.

IR780 based nanomaterials have been by far the most explored for cancer theragnostic. This fact can be explained

Table 4. In vivo therapeutic performance of Cypate based nanostructures.

Cypate based nanostructures	Phototherapy modality	Tumor model	Administration route	Dose[a]	Laser parameters	Other therapeutic molecules	Therapeutic effect	Ref.
Cypate loaded HA based nanoparticles	PTT/PDT	MCF-7 tumor bearing mice	i.v.	40 μg	785 nm; 0.5 W cm^{-2}; 5 min	–	Tumor eradication	[43]
Cypate-BSA based nanoparticles	PTT	4T1 tumor bearing mice	i.v.	1.5 mg kg^{-1}	785 nm; 1.5 W cm^{-2}; 3 min	–	Tumor eradication	[54]
PEG-Cypate micelles	PTT/PDT	B16F10 tumor bearing mice	i.v.	5 mg kg^{-1}	808 nm; 0.4 W cm^{-2}; 10 min	–	Tumor eradication	[57]
Cypate-PEG- GO	PTT	4T1 tumor bearing mice	i.v.	7.5 mg kg^{-1}	785 nm; 1.0 W cm^{-2}; 3 min	GO	Tumor eradication	[114]
Cypate and PTX loaded PEGylated nanoparticles[b]	PTT	4T1 tumor bearing mice	i.v.	7.5 mg kg^{-1}	785 nm; 1.0 W cm^{-2}; 5 min	PTX	Tumor eradication	[56]
Cypate and 17AAG loaded PEGylated micelles[c]	PTT/PDT	A549 tumor bearing mice	i.v.	7.5 mg kg^{-1} (3 times)	785 nm; 1.5 W cm^{-2}; 3 min (3 times)	17AAG	Tumor eradication	[113]
Cypate and Pt(IV) prodrug loaded PEGylated micelles[d]	PTT/PDT	A549R tumor bearing mice	i.v.	7.5 mg kg^{-1} (3 times)	785 nm; 1.5 W cm^{-2}; 3 min (3 times)	Pt(IV) prodrug	Tumor eradication	[55]
DOX loaded PEGylated Cypate- mesoporous silica nanoparticles	PTT/PDT	4T1 tumor bearing mice	i.v.	8.5 mg kg^{-1}	785 nm; 1.5 W cm^{-2}; 5 min (twice)	DOX	Tumor eradication	[116]
HA coated Melittin/ Cypate nanoagents	PTT	4T1 tumor bearing mice	i.v.	3 mg kg^{-1}	808 nm; 1.0 W cm^{-2}; 10 min	Melittin	Tumor regression	[36]
DTX loaded iRGD-Cypate- PAMAM dendrimers	PTT/PDT	HepG2 tumor bearing mice	i.v.	6.7 mg kg^{-1} (every 5 days)	808 nm; 1.6 W cm^{-2}; 5 min (every 5 days)	DTX	Tumor regression	[32]
Cypate and DPAE loaded PEGylated micelles[e]	PTT/PDT	4T1 tumor bearing mice	i.v.	7.5 mg kg^{-1} (twice)	808 nm; 1.5 W cm^{-2}; 5 min	DPAE	Tumor regression	[112]
Cypate and DOX loaded PEGylated liposomes[f]	PTT	4T1 tumor bearing mice	i.t.	10 mg kg^{-1} of DOX	785 nm; 1.6 W cm^{-2}; 5 min	DOX	Tumor regression	[133]
Cypate loaded PEGylated micelles[d]	PTT	A549 tumor bearing mice	i.v.	10 mg kg^{-1} (3 times)	785 nm; 1.0 W cm^{-2}; 5 min (3 times)	–	Tumor regression	[117]
PEGylated Cypate and DOX based micelles[g]	PTT	MCF-7/ADR tumor bearing mice	i.v.	10 mg kg^{-1} (3 times)	808 nm; 16 W cm^{-2}; 2 min (3 times)	DOX	Tumor growth inhibition	[58]
Cypate-silk fibroin nanoparticles	PTT	K7M2 tumor bearing mice	i.v.	10 μg of nanostructures	808 nm; 0.75 W cm^{-2}; 10 min	–	Tumor growth reduction	[134]
Cypate and Ce6 loaded PEGylated micelles[d]	PTT/PDT	4T1 tumor bearing mice	i.v.	7.5 mg kg^{-1} (3 times)	785 nm; 1.0 W cm^{-2}; 5 min 660 nm; 1.0 W cm^{-2}; 10 min (3 times)	Ce6	Tumor growth reduction	[115]
DOX loaded TPGS coated Cypate-mesoporous silica nanoparticles	PTT	4T1 tumor bearing mice	i.v.	10 mg kg^{-1} of DOX (3 times)	808 nm; 2.0 W cm^{-2}; 2 min (3 times)	DOX TPGS	Tumor growth reduction	[135]

[a]Dose of heptamethine cyanine (unless stated otherwise); [b]formulated with PEG-PCL-SS-P(NIPAM-*co*-DMA); [c]formulated with PEG-PCL; [d]formulated with mPEG-PAsp(DA); [e]formulated with PEG-PCL-poly((2-(piperidin-1-yl) ethyl methacrylate); [f]formulated with DPPC, cholestherol, DSPE-PEG and NH_4HCO_3; [g]formulated with a PEGylated Cypate amphiphilic conjugate and Pluronic P123-DOX based conjugate.

Table 5. In vivo therapeutic performance of IR808 based nanostructures.

IR808 based nanostructures	Phototherapy modality	Tumor model	Administration route	Dose[a)]	Laser parameters	Other therapeutic molecules	Therapeutic effect	Ref.
IR808-PEG-DSPE coated SPIONs	PTT	SCC7 tumor bearing mice	i.t.	N.D.	808 nm; 1.0 W cm^{-2}; 10 min	–	Tumor eradication	[120]
IR808-HA nanoparticles	PTT	A549 tumor bearing mice	i.v.	36 μg	808 nm; 0.8 W cm^{-2}; 5 min	–	Tumor eradication	[30]
IR808-PEG-PSMA[b)] coated MnO nanoparticles	PTT/PDT	MCF-7 tumor bearing mice	i.v.	50 μg	808 nm; 0.5 W cm^{-2}; 5 min	MnO nanoparticles	Tumor eradication	[37]
IR808-PEI-PEG-GO	PTT/PDT	A549 or Lewis tumor bearing mice	i.v.	10 mg kg^{-1} of nanostructures	808 nm; 1.0 W cm^{-2}; 5 min	GO	Tumor eradication	[21]
PTX loaded IR808-HGC[c)] micelles	PTT	SCC7 tumor bearing mice	i.t.	10 mg kg^{-1} of nanostructures	808 nm; 1.0 W cm^{-2}; 5 min	PTX	Tumor regression	[119]

[a)]Dose of heptamethine cyanine (unless stated otherwise); [b)]cumene terminated poly (styrene-*co*-maleic anhydride); [c)]5β-cholanic acid-glycol chitosan conjugate.

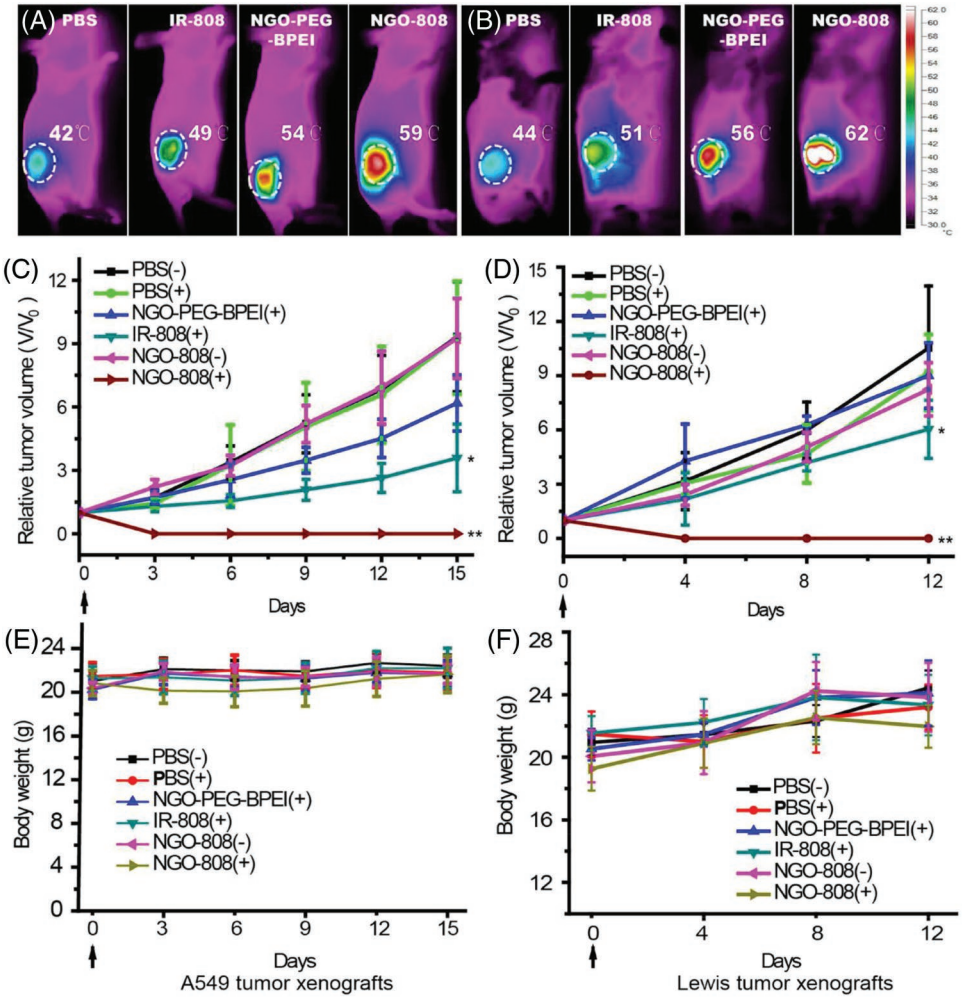

Figure 4. PTT/PDT mediated by IR808-PEI-PEG-GO. Thermal images of A) A549 and B) Lewis tumor bearing mice after the different treatments. C,D) Tumor volume and E,F) body weight changes of after the different treatments. PBS (–): PBS; PBS (+): PBS + NIR radiation; NGO-PEG-BPEI (+): PEI-PEG-GO + NIR radiation; IR808 (+): IR808 + NIR radiation; NGO-808 (–): IR808-PEI-PEG-GO; NGO-808 (+): IR808-PEI-PEG-GO + NIR radiation; NIR radiation: 808 nm; 1.0 W cm^{-2}; 5 min. Reproduced with permission.[21] Copyright 2016, American Chemical Society.

Table 6. In vivo therapeutic performance of IR820 based nanostructures.

IR820 based nanostructures	Phototherapy modality	Tumor model	Administration route	Dose[a]	Laser parameters	Other therapeutic molecules	Therapeutic effect	Ref.
IR820 and Tanespimycin loaded liposomes[b]	PTT/PDT	SCC-7 tumor bearing mice	i.t.	50 μg	808 nm; 2.0 W cm^{-2}; 3 min 660 nm; 0.2 W cm^{-2}; 3 min	Tanespimycin	Tumor eradication	[136]
IR820 loaded ferritin nanocages	PTT	4T1 tumor bearing mice	i.v.	400 μg	808 nm; 0.5 W cm^{-2}; 10 min	–	Tumor eradication	[60]
IR820 and DTX loaded micelles[c]	PTT/PDT	4T1 tumor bearing mice	i.v.	2 mg kg^{-1} (3 times)	808 nm; 2.5 W cm^{-2}; 10 min (3 times)	DTX	Tumor eradication	[63]
PEGylated IR820-conjugated poly(β-amine ester) and ZnPP[d]-poly(β-amine ester) micelles	PTT	A549 tumor bearing mice	i.v.	5 mg kg^{-1} of nanostructures (3 times)	808 nm; 1.0 W cm^{-2}; 10 min (3 times)	ZnPP	Tumor eradication	[7]
IR820 and Bortezomib loaded Cyclosporine A-functionalized PEG-coated mesoporous silica nanoparticles[e]	PTT	PANC-1 tumor bearing mice	i.v.	N.D. (4 times)	808 nm; 3.0 W cm^{-2}; 5 min (4 times)	Bortezomib	Tumor regression	[137]
IR820 loaded PLGA nanoparticles	PTT	MDA-MB-231 tumor bearing mice	i.v.	0.035 μmol (4 times)	810 nm; 1.5 W cm^{-2}; 5 min (4 times)	–	Tumor regression	[62]
IR820 loaded PEGylated liposomes[f]	PTT	C6 tumor bearing mice	i.v.	10 mg kg^{-1} of nanostructures	808 nm; 1.0 W cm^{-2}; 15 min	–	Tumor regression	[138]
IR820 and Irinotecan loaded hollow mesoporous silica nanoparticles	PTT	EMT6 tumor bearing mice	intraperitoneal (i.p.)	3 mg kg^{-1} (4 times)	808 nm; 2.0 W cm^{-2}; 5 min (4 times)	Irinotecan	Tumor regression	[139]
IR820-ELP[g] micelles	PTT	CT-26 tumor bearing mice	i.v.	N.D.	808 nm; 1.5 W cm^{-2}; 8 min	–	Tumor growth reduction	[31]
IR820 loaded TPP-targeted PEGylated GO[h] incorporating CpG	PTT/PDT	EMT6 tumor bearing mice	i.t.	20 μg	808 nm; 0.5 W cm^{-2}; 5 min	CpG GO	Tumor growth reduction	[140]
IR820-PTX nanoparticles	PTT	4T1 tumor bearing mice	i.v.	4.2 mg kg^{-1} of nanostructures (every 3 days)	660 nm; 1.0 W cm^{-2}; 5 min (every 3 days)	PTX	Tumor growth reduction	[61]
Ce6 loaded IR820-TPGS micelles	PTT/PDT	B16 tumor bearing mice	i.v.	8 mg kg^{-1} (every 3 days)	660 nm; 1.0 W cm^{-2}; 5 min (every 3 days)	Ce6	Tumor growth reduction	[59]

[a]Dose of heptamethine cyanine (unless stated otherwise); [b]formulated with DSPE-PEG, DPPC and cholesterol; [c]formulated with mPEG-PCL and PCL-PEI-PEG-(Lyp-1); [d]zinc protoporphyrin; [e]coated with DPPC, CHO, DSPE-PEG, and DSPE-PEG-(Cyclosporine A); [f]formulated with DSPE-PEG, DPPC, DSPC; [g]elastin like polypeptide; [h]coated with DSPE-PEG-TPP and DSPE-PEG-(cytosine-phosphate-guanine oligodeoxynucleotides) (CpG).

by the high molar extinction coefficient and singlet oxygen quantum yield of IR780. In several reports, IR780 based nanomaterials mediated tumors eradication upon NIR laser irradiation, thereby demonstrating a great potential for cancer PTT/PDT. Furthermore, these nanostructures also displayed the capacity to detect tumors by NIR fluorescence imaging and PAI. On the other hand, nanostructures incorporating IR808, IR820, IR825, and Cypate have not been as extensively explored for cancer phototheragnostic. In the case of IR808, IR825 and Cypate, such could be related to the fact that these dyes are not yet commercially available from the most popular chemical suppliers. Still, the studies reported so far suggest their good potential for cancer PTT/PDT and imaging, as evidenced by the ability of some formulations to photo-ablate tumors.

Regarding nanomaterials incorporating IR775, IR797, and IR806, the information available in the literature on their applicability for in vivo cancer phototheragnostic makes it too preliminary to conclude about their potential. In the case of IR783 and IRDye 800CW based nanomaterials, only studies

Table 7. In vivo therapeutic performance of IR825 based nanostructures.

IR825 based nanostructures	Phototherapy modality	Tumor model	Administration route	Dose[a]	Laser parameters	Other therapeutic molecules	Therapeutic effect	Ref.
HSA-IR825 nanoparticles	PTT	4T1 tumor bearing mice	i.v.	26 μg	808 nm; 0.8 W cm^{-2}; 10 min	–	Tumor eradication	[141]
PEG-PDA coated Mn-IR825 nanoparticles	PTT	4T1 tumor bearing mice	i.v.	100 μg	808 nm; 0.6 W cm^{-2}; 5 min	PDA	Tumor eradication	[142]
IR825 loaded PEG-PMAO micelles	PTT	4T1 tumor bearing mice	i.v.	200 μg of nanostructures	808 nm; 0.5 W cm^{-2}; 5 min	–	Tumor eradication	[39]
IR825 and IONPs[c] loaded PEG-PAA-PAH[d] nanoparticles	PTT	4T1 tumor bearing mice	i.v.	200 μg of nanostructures	915 nm; 0.7 W cm^{-2}; 5 min	IONPs	Tumor eradication	[27]
dc-IR825 and 17AAG loaded HSA nanoparticles	PTT/PDT	4T1 tumor bearing mice	i.v.	1 mg kg^{-1}	808 nm; 0.3 W cm^{-2}; 10 min	17AAG	Tumor eradication	[64]
dc-IR825 loaded TPGS micelles	PTT/PDT	U14 tumor bearing mice	i.v.	3 mg kg^{-1}	808 nm; 0.3 W cm^{-2}; 10 min	TPGS	Tumor eradication	[65]
mPEG-*b*-PLD[e]-IR825[b] conjugate micelles	PTT	U14 tumor bearing mice	i.v.	10 mg kg^{-1} of nanostructures	808 nm; 1.0 W cm^{-2}; 10 min	–	Tumor eradication	[46]
me-IR825 loaded Pluronic F-127 based nanoparticles	PTT	U14 tumor bearing mice	i.v.	300 mg kg^{-1} of nanostructures	808 nm; 1.0 W cm^{-2}; 10 min	–	Tumor eradication	[66]
PFOB loaded HA-IR825 nanoparticles	PTT	HT-29 tumor bearing mice	i.v.	500 μg of nanostructures	808 nm; 1.5 W cm^{-2}; 10 min	PFOB	Tumor regression	[125]
IR825 and CA4[f] loaded siHSP70[g]/PEI-PLA micelles	PTT	MDA-MB-231 tumor bearing mice	i.v.	5 mg kg^{-1} of CA4	808 nm; 0.5 W cm^{-2}; 5 min	CA4 siHSP70	Tumor regression	[123]
IR825 loaded carbonized cross-linked PEG-*g*-poly(sulfobetaine methacrylate) nanoparticles	PTT	MDA-MB-231 tumor bearing mice	i.v.	10 mg kg^{-1} of nanostructures	808 nm; 2.0 W cm^{-2}; 5 min	–	Tumor regression	[143]
IR825 loaded PEG-*g*-(formyl benzoic acid/cysteamine/bromoethyl amine)-conjugated poly(DMA[h]-*co*-HEMA[i]) nanoparticles	PTT	MDA-MB-231 tumor bearing mice	subcutaneous (s.c.)	10 mg kg^{-1} of nanostructures	808 nm; 2.0 W cm^{-2}; 5 min	–	Tumor regression	[144]
IR825 and DOX loaded PEG-PAA-PEI aggregates	PTT	4T1 tumor bearing mice	i.v.	13 mg kg^{-1}	915 nm; 0.35 W cm^{-2}; 20 min	DOX	Tumor regression	[124]
PEG-IR825[j] and HA-PDA anchored rGO[k]	PTT	MDA-MB-231 tumor bearing mice	i.v.	30 mg kg^{-1} of nanostructures	808 nm; 2.0 W cm^{-2}; 5 min	PDA rGO	Tumor regression	[127]
IR825 loaded TCPP cross-linked PEGylated micelles[l]	PTT/PDT	4T1 tumor bearing mice	i.v.	100 μg	808 nm; 0.8 W cm^{-2}; 5 min 660 nm; 5 mW cm^{-2}; 60 min	TCPP	Tumor growth reduction	[33]
IR825 loaded CPT-adamantine β-cyclodextrin-HA nanoparticles	PTT	U14 tumor bearing mice	i.v.	200 μg of nanostructures	808 nm; 0.5 W cm^{-2}; 5 min	CPT	Tumor growth reduction	[145]
IR825 and RB[m] loaded BSA-PAA coated UCNPs[n]	PTT/PDT	4T1 tumor bearing mice	i.t.	400 μg of nanostructures	808 nm; 0.5 W cm^{-2}; 5 min 980 nm; 0.4 W cm^{-2}; 30 min	RB	Tumor growth reduction	[146]

[a]Dose of heptamethine cyanine (unless stated otherwise); [b]IR825 derivative modified with a primary amine; [c]iron oxide nanoparticles; [d]poly(allylamine hydrochloride); [e]poly(L-aspartic acid sodium salt); [f]combretastatin A4; [g]HSP70 siRNA; [h]2-(dimethylamino)ethyl methacrylate; [i]2-hydroxyethyl methacrylate; [j]IR825 and 2-chloro-3′,4′-dihydroxyacetophenone quaternized PEG-*g*-poly(dimethylaminoethyl methacrylate); [k]reduced graphene oxide; [l]formulated with poly[(PEG methyl ether methacrylate)-*co*-(3-aminopropyl methacrylate)]-*b*-poly(methyl methacrylate); [m]rose bengal; [n]upconversion nanoparticles.

Table 8. In vivo therapeutic performance of other heptamethine cyanine based nanostructures.

Other heptamethine cyanine based nanostructures	Phototherapy modality	Tumor model	Administration route	Dose[a)]	Laser parameters	Other therapeutic molecules	Therapeutic effect	Ref.
IR797 loaded PEG-PMAO micelles	PTT	HeLa tumor bearing mice	i.t.	1.05 µmol	808 nm; 1.0 W cm^{-2}; 5 min	–	Tumor eradication	[67]
PEGylated IR806 coated IONPs micelles[b)]	PTT	LLC tumor bearing mice	i.v.	N.D.	808 nm; 0.25 W cm^{-2}; 20 min	IONPs	Tumor regression	[147]
IR775 loaded mPEG-PCL nanoparticles	PTT/PDT	A2780/ CDDP tumor bearing mice	i.v.	0.75 mg kg^{-1}	785 nm; 1.0 W cm^{-2}; 20 min	–	Tumor growth reduction	[10]
IR806-PEG-DSPE coated $MnFe_2O_4$ nanoparticles	PTT/PDT	H22 tumor bearing mice	i.v.	0.92 mg kg^{-1}	808 nm; 1.0 W cm^{-2}; 5 min	$MnFe_2O_4$ nanoparticles	Tumor growth reduction	[68]

[a)]Dose of heptamethine cyanine (unless stated otherwise); [b)]prepared by functionalizing IR808 coated IONPs with an mPEG-PCL-(NH_2-terminated dendritic polyamidoamine) (PAMAM)-based amphiphile.

demonstrating their applicability for in vivo tumor imaging have been reported so far. In this way, developing new formulations containing these NIR heptamethine cyanines will be crucial to prove their applicability for cancer phototheragnostic. The same should be performed for FD-1080 since at the present time, nanoformulations containing this prototypic NIR absorbing heptamethine cyanines have not yet been developed.

In general, the therapeutic capacity of the prototypic NIR heptamethine cyanine incorporating nanomaterials could be further improved through the inclusion of other therapeutic agents (e.g., chemotherapeutics, photosensitizers, or photothermal agents) in the nanoformulations. This strategy also enabled combinatorial phototherapies using lower doses and/or less intense laser irradiations.

Currently, there are several ongoing clinical trials (phase I and II) studying the diagnosis capabilities of antibody-IRDye 800CW conjugates (e.g., Bevacizumab-IRDye 800CW). However, the clinical translation of phototheragnostics based on nanomaterials incorporating prototypic NIR heptamethine cyanines has not yet been accomplished. Before envisioning the use of heptamethine cyanine incorporating nanomaterials in clinical trials, it is fundamental to determine their long-term toxicity and confirm their theragnostic capacities in large animal models. Furthermore, the practical use of nanomaterials incorporating prototypic NIR heptamethine cyanines for cancer phototheragnostics is strongly circumscribed to superficial cancers (e.g., melanoma, breast cancer) due to the limits imposed by the penetration depth of the NIR radiation. In this context, phototheragnostics in the second-NIR window (1000–1350 nm) can achieve a higher penetration depth (due to reduced light scattering) and higher maximal permissible exposure (due to the lower energy of longer wavelength photons).[73] Among the different heptamethine cyanines, only FD-1080 has optical properties that enable its efficient use in the second-NIR window. To surpass this bottleneck, endoscopes coupled with fiber-type NIR lasers (e.g., 808 nm) are promising devices that may enable the use of nanomaterials incorporating prototypic NIR heptamethine cyanines for the imaging and PTT/PDT of nonsuperficial tumors.[74]

Overall, the continuous development of nanomaterials incorporating the prototypic NIR absorbing heptamethine cyanines will cement their phototheragnostic capabilities.

Acknowledgements

M.M.L., D.d.M.-D., and C.G.A. contributed equally to this work. This work was supported by European Regional Development Fund and FEDER funds through the POCI-COMPETE 2020-Operational Programme Competitiveness and Internationalisation in Axis I-Strengthening research, technological development and innovation (Project POCI-01-0145-FEDER-007491, CENTRO-01-0145-FEDER-028989, and POCI-01-0145-FEDER-031462) and National Funds by FCT-Foundation for Science and Technology (Project UID/Multi/00709/2013). D.d.M.-D. acknowledges CENTRO-01-0145-FEDER-028989 for the funding given on the form of a research contract. C.G.A. and R.L.-S. acknowledge funding from the grant UBI-Santander/Totta and individual Ph.D. fellowships from FCT (SFRH/BD/145386/2019 and SFRH/BD/144922/2019).

Conflict of Interest

The authors declare no conflict of interest.

Keywords

cancer, heptamethine cyanines, NIR imaging, photoacoustic imaging, phototherapies

Received: November 21, 2019
Revised: January 16, 2020
Published online:

[1] a) A. Sneider, D. VanDyke, S. Paliwal, P. Rai, *Nanotheranostics* **2017**, *1*, 1; b) X. Song, Q. Chen, Z. Liu, *Nano Res.* **2015**, *8*, 340; c) P. Zhang, C. Hu, W. Ran, J. Meng, Q. Yin, Y. Li, *Theranostics* **2016**, *6*, 948.

[2] Y. Cai, W. Si, W. Huang, P. Chen, J. Shao, X. Dong, *Small* **2018**, *14*, 1704247.
[3] a) C. G. Alves, R. Lima-Sousa, D. de Melo-Diogo, R. O. Louro, I. J. Correia, *Int. J. Pharm. (Amsterdam, Neth.)* **2018**, *542*, 164; b) D. de Melo-Diogo, R. Lima-Sousa, C. G. Alves, I. J. Correia, *Biomater. Sci.* **2019**, *7*, 3534; c) D. de Melo-Diogo, E. C. Costa, C. G. Alves, R. Lima-Sousa, P. Ferreira, R. O. Louro, I. J. Correia, *Eur. J. Pharm. Biopharm.* **2018**, *131*, 162.
[4] a) Y. Chen, L. Li, W. Chen, H. Chen, J. Yin, *Chin. Chem. Lett.* **2019**, *30*, 1353; b) D. de Melo-Diogo, C. Pais-Silva, E. C. Costa, R. O. Louro, I. J. Correia, *Nanomedicine* **2017**, *12*, 443.
[5] D. de Melo-Diogo, C. Pais-Silva, D. R. Dias, A. F. Moreira, I. J. Correia, *Adv. Healthcare Mater.* **2017**, *6*, 1700073.
[6] F. Yan, W. Duan, H. W. Yekuo Li, Y. Zhou, M. Pan, H. Liu, X. Liu, H. Zheng, *Theranostics* **2016**, *6*, 2337.
[7] J. Noh, E. Jung, D. Yoo, C. Kang, C. Kim, S. Park, G. Khang, D. Lee, *ACS Appl. Mater. Interfaces* **2018**, *10*, 40424.
[8] a) R. Lima-Sousa, D. de Melo-Diogo, C. G. Alves, E. C. Costa, P. Ferreira, R. O. Louro, I. J. Correia, *Carbohydr. Polym.* **2018**, *200*, 93; b) A. F. Moreira, D. R. Dias, E. C. Costa, I. J. Correia, *Eur. J. Pharm. Sci.* **2017**, *104*, 42; c) Y.-W. Jiang, G. Gao, P. Hu, J.-B. Liu, Y. Guo, X. Zhang, X.-W. Yu, F.-G. Wu, X. Lu, *Nanoscale* **2020**, *12*, 210; d) Y.-W. Bao, X.-W. Hua, X. Chen, F.-G. Wu, *Biomaterials* **2018**, *183*, 30; e) G. Gao, Y.-W. Jiang, H.-R. Jia, W. Sun, Y. Guo, X.-W. Yu, X. Liu, F.-G. Wu, *Biomaterials* **2019**, *223*, 119443; f) W. Sun, X. Zhang, H. R. Jia, Y. X. Zhu, Y. Guo, G. Gao, Y. H. Li, F. G. Wu, *Small* **2019**, *15*, 1804575.
[9] X. Chen, X. Zhang, Y. Guo, Y. X. Zhu, X. Liu, Z. Chen, F. G. Wu, *Adv. Funct. Mater.* **2019**, *29*, 1807772.
[10] T. Duong, X. Li, B. Yang, C. Schumann, H. A. Albarqi, O. Taratula, O. Taratula, *Nanomedicine (N. Y., NY, U. S.)* **2017**, *13*, 955.
[11] J. Weber, P. C. Beard, S. E. Bohndiek, *Nat. Methods* **2016**, *13*, 639.
[12] L. Wu, S. Fang, S. Shi, J. Deng, B. Liu, L. Cai, *Biomacromolecules* **2013**, *14*, 3027.
[13] C. Shi, J. B. Wu, D. Pan, *J. Biomed. Opt.* **2016**, *21*, 1.
[14] E.-H. Lee, S.-J. Lim, M.-K. Lee, *Carbohydr. Polym.* **2019**, *224*, 115143.
[15] S. Zhu, R. Tian, A. L. Antaris, X. Chen, H. Dai, *Adv. Mater.* **2019**, *31*, 1900321.
[16] a) Z. Sheng, D. Hu, M. Xue, M. He, P. Gong, L. Cai, *Nano-Micro Lett.* **2013**, *5*, 145; b) H. Wang, X. Li, B. W.-C. Tse, H. Yang, C. A. Thorling, Y. Liu, M. Touraud, J. B. Chouane, X. Liu, M. S. Roberts, *Theranostics* **2018**, *8*, 1227; c) A. Raza, U. Hayat, T. Rasheed, M. Bilal, H. M. Iqbal, *J. Mater. Res. Technol.* **2019**, *8*, 1497.
[17] a) U. Bazylińska, A. Lewińska, Ł. Lamch, K. A. Wilk, *Colloids Surf., A* **2014**, *442*, 42; b) K. Kiyose, S. Aizawa, E. Sasaki, H. Kojima, K. Hanaoka, T. Terai, Y. Urano, T. Nagano, *Chem. - Eur. J.* **2009**, *15*, 9191.
[18] N. S. James, Y. Chen, P. Joshi, T. Y. Ohulchanskyy, M. Ethirajan, M. Henary, L. Strekowsk, R. K. Pandey, *Theranostics* **2013**, *3*, 692.
[19] K. Licha, B. Riefke, V. Ntziachristos, A. Becker, B. Chance, W. Semmler, *Photochem. Photobiol.* **2000**, *72*, 392.
[20] T. Jing, L. Fu, L. Liu, L. Yan, *Polym. Chem.* **2016**, *7*, 951.
[21] S. Luo, Z. Yang, X. Tan, Y. Wang, Y. Zeng, Y. Wang, C. Li, R. Li, C. Shi, *ACS Appl. Mater. Interfaces* **2016**, *8*, 17176.
[22] N. Zhao, C. Zhang, Y. Zhao, B. Bai, J. An, H. Zhang, J. B. Wu, C. Shi, *Oncotarget* **2016**, *7*, 57277.
[23] E. Zhang, S. Luo, X. Tan, C. Shi, *Biomaterials* **2014**, *35*, 771.
[24] X. Yang, C. Shi, R. Tong, W. Qian, H. E. Zhau, R. Wang, G. Zhu, J. Cheng, V. W. Yang, T. Cheng, *Clin. Cancer Res.* **2010**, *16*, 2833.
[25] X. Tan, S. Luo, D. Wang, Y. Su, T. Cheng, C. Shi, *Biomaterials* **2012**, *33*, 2230.
[26] A. Yuan, X. Qiu, X. Tang, W. Liu, J. Wu, Y. Hu, *Biomaterials* **2015**, *51*, 184.
[27] X. Song, H. Gong, T. Liu, L. Cheng, C. Wang, X. Sun, C. Liang, Z. Liu, *Small* **2014**, *10*, 4362.
[28] M. V. Marshall, D. Draney, E. M. Sevick-Muraca, D. M. Olive, *Mol. Imaging Biol.* **2010**, *12*, 583.
[29] Y. Liu, P. Bhattarai, Z. Dai, X. Chen, *Chem. Soc. Rev.* **2019**, *48*, 2053.
[30] S. Li, Z. Sun, G. Deng, X. Meng, W. Li, D. Ni, J. Zhang, P. Gong, L. Cai, *Biomater. Sci.* **2017**, *5*, 1122.
[31] K. Huang, M. Gao, L. Fan, Y. Lai, H. Fan, Z. Hua, *Biomater. Sci.* **2018**, *6*, 2925.
[32] R. Ge, J. Cao, J. Chi, S. Han, Y. Liang, L. Xu, M. Liang, Y. Sun, *Int. J. Nanomed.* **2019**, *14*, 4931.
[33] X. Liu, G. Yang, L. Zhang, Z. Liu, Z. Cheng, X. Zhu, *Nanoscale* **2016**, *8*, 15323.
[34] C. G. Alves, D. de Melo-Diogo, R. Lima-Sousa, E. C. Costa, I. J. Correia, *Eur. J. Pharm. Biopharm.* **2019**, *137*, 86.
[35] C. Pais-Silva, D. de Melo-Diogo, I. J. Correia, *Eur. J. Pharm. Biopharm.* **2017**, *113*, 108.
[36] H.-R. Jia, Y.-X. Zhu, X. Liu, G.-Y. Pan, G. Gao, W. Sun, X. Zhang, Y.-W. Jiang, F.-G. Wu, *ACS Nano* **2019**, *13*, 11781.
[37] L. Zhou, Y. Wu, X. Meng, S. Li, J. Zhang, P. Gong, P. Zhang, T. Jiang, G. Deng, W. Li, *Small* **2018**, *14*, 1801008.
[38] M. Liu, P. Zhang, L. Deng, D. Guo, M. Tan, J. Huang, Y. Luo, Y. Cao, Z. Wang, *Biomater. Sci.* **2019**, *7*, 1132.
[39] L. Cheng, W. He, H. Gong, C. Wang, Q. Chen, Z. Cheng, Z. Liu, *Adv. Funct. Mater.* **2013**, *23*, 5893.
[40] Y. Zhang, C. Y. Ang, M. Li, S. Y. Tan, Q. Qu, Y. Zhao, *ACS Appl. Mater. Interfaces* **2016**, *8*, 6869.
[41] B. Xia, B. Wang, Z. Chen, Q. Zhang, J. Shi, *Adv. Mater. Interfaces* **2016**, *3*, 1500715.
[42] a) A. Fernandez-Fernandez, R. Manchanda, D. A. Carvajal, T. Lei, A. J. McGoron, in *Proc. SPIE 8596, Reporters, Markers, Dyes, Nanoparticles, and Molecular Probes for Biomedical Applications V*, SPIE, Bellingham, WA **2013**, 859605; b) Y. Matsumoto, J. W. Nichols, K. Toh, T. Nomoto, H. Cabral, Y. Miura, R. J. Christie, N. Yamada, T. Ogura, M. R. Kano, Y. Matsumura, N. Nishiyama, T. Yamasoba, Y. H. Bae, K. Kataoka, *Nat. Nanotechnol.* **2016**, *11*, 533.
[43] Y. Tian, R. Guo, Y. Wang, W. Yang, *Adv. Healthcare Mater.* **2016**, *5*, 3099.
[44] H. Chen, B. Li, J. Qiu, J. Li, J. Jin, S. Dai, Y. Ma, Y. Gu, *Nanoscale* **2013**, *5*, 12409.
[45] a) D. de Melo-Diogo, R. Lima-Sousa, C. G. Alves, E. C. Costa, R. O. Louro, I. J. Correia, *Colloids Surf., B* **2018**, *171*, 260; b) A. F. Moreira, D. R. Dias, I. J. Correia, *Microporous Mesoporous Mater.* **2016**, *236*, 141; c) S. Wilhelm, A. J. Tavares, Q. Dai, S. Ohta, J. Audet, H. F. Dvorak, W. C. W. Chan, *Nat. Rev. Mater.* **2016**, *1*, 16014; d) M. F. Attia, N. Anton, J. Wallyn, Z. Omran, T. F. Vandamme, *J. Pharm. Pharmacol.* **2019**, *71*, 1185; e) C. F. Rodrigues, T. A. Jacinto, A. F. Moreira, E. C. Costa, S. P. Miguel, I. J. Correia, *Nano Res.* **2019**, *12*, 719.
[46] G.-Y. Pan, H.-R. Jia, Y.-X. Zhu, F.-G. Wu, *Nanoscale* **2018**, *10*, 2115.
[47] J. Song, N. Zhang, L. Zhang, H. Yi, Y. Liu, Y. Li, X. Li, M. Wu, L. Hao, Z. Yang, Z. Wang, *Int. J. Nanomed.* **2019**, *14*, 2757.
[48] S. Xiang, K. Zhang, G. Yang, D. Gao, C. Zeng, M. He, *Nanoscale Res. Lett.* **2019**, *14*, 211.
[49] Q. Yang, Y. Xiao, Y. Yin, G. Li, J. Peng, *Mol. Pharmaceutics* **2019**, *16*, 7.
[50] X. Wang, J. Yan, D. Pan, R. Yang, L. Wang, Y. Xu, J. Sheng, Y. Yue, Q. Huang, Y. Wang, R. Wang, M. Yang, *Adv. Healthcare Mater.* **2018**, *7*, 1701505.
[51] S. Wang, F. Guo, Y. Ji, M. Yu, J. Wang, N. Li, *Mol. Pharmaceutics* **2018**, *15*, 3318.
[52] X. Yang, H. Li, C. Qian, Y. Guo, C. Li, F. Gao, Y. Yang, K. Wang, D. Oupicky, M. Sun, *Nanomedicine (N. Y., NY, U. S.)* **2018**, *14*, 2283.

[53] Z. Yang, R. Cheng, C. Zhao, N. Sun, H. Luo, Y. Chen, Z. Liu, X. Li, J. Liu, Z. Tian, *Theranostics* **2018**, *8*, 4097.
[54] Y. Wang, T. Yang, H. Ke, A. Zhu, Y. Wang, J. Wang, J. Shen, G. Liu, C. Chen, Y. Zhao, *Adv. Mater.* **2015**, *27*, 3874.
[55] Y. Li, Y. Deng, X. Tian, H. Ke, M. Guo, A. Zhu, T. Yang, Z. Guo, Z. Ge, X. Yang, *ACS Nano* **2015**, *9*, 9626.
[56] X. An, A. Zhu, H. Luo, H. Ke, H. Chen, Y. Zhao, *ACS Nano* **2016**, *10*, 5947.
[57] W. Miao, H. Kim, V. Gujrati, J. Y. Kim, H. Jon, Y. Lee, M. Choi, J. Kim, S. Lee, D. Y. Lee, *Theranostics* **2016**, *6*, 2367.
[58] H. Yu, Z. Cui, P. Yu, C. Guo, B. Feng, T. Jiang, S. Wang, Q. Yin, D. Zhong, X. Yang, *Adv. Funct. Mater.* **2015**, *25*, 2489.
[59] X. Hu, H. Tian, W. Jiang, A. Song, Z. Li, Y. Luan, *Small* **2018**, *14*, 1802994.
[60] P. Huang, P. Rong, A. Jin, X. Yan, M. G. Zhang, J. Lin, H. Hu, Z. Wang, X. Yue, W. Li, *Adv. Mater.* **2014**, *26*, 6401.
[61] D. Zhang, J. Zhang, Q. Li, H. Tian, N. Zhang, Z. Li, Y. Luan, *ACS Appl. Mater. Interfaces* **2018**, *10*, 30092.
[62] D. M. Valcourt, M. N. Dang, E. S. Day, *J. Biomed. Mater. Res., Part A* **2019**, *107*, 1702.
[63] W. Li, J. Peng, L. Tan, J. Wu, K. Shi, Y. Qu, X. Wei, Z. Qian, *Biomaterials* **2016**, *106*, 119.
[64] G. Gao, Y. W. Jiang, W. Sun, Y. Guo, H. R. Jia, X. W. Yu, G. Y. Pan, F. G. Wu, *Small* **2019**, *15*, 1900501.
[65] Y.-X. Zhu, H.-R. Jia, G. Gao, G.-Y. Pan, Y.-W. Jiang, P. Li, N. Zhou, C. Li, C. She, N. W. Ulrich, *Biomaterials* **2019**, *232*, 119668.
[66] G.-Y. Pan, H.-R. Jia, Y.-X. Zhu, W. Sun, X.-T. Cheng, F.-G. Wu, *ACS Appl. Nano Mater.* **2018**, *1*, 2885.
[67] Y. F. Xiao, F. F. An, J. X. Chen, J. Yu, W. W. Tao, Z. Yu, R. Ting, C. S. Lee, X. H. Zhang, *Small* **2019**, *15*, 1903121.
[68] K. Deng, Y. Chen, C. Li, X. Deng, Z. Hou, Z. Cheng, Y. Han, B. Xing, J. Lin, *J. Mater. Chem. B* **2017**, *5*, 1803.
[69] B. Zhang, H. Wang, S. Shen, X. She, W. Shi, J. Chen, Q. Zhang, Y. Hu, Z. Pang, X. Jiang, *Biomaterials* **2016**, *79*, 46.
[70] J. Feng, S. Li, H.-J. Fan, Y. Lin, Y. Lu, *Colloids Surf., B* **2019**, *178*, 146.
[71] L. Li, T. L. M. ten Hagen, M. Bolkestein, A. Gasselhuber, J. Yatvin, G. C. van Rhoon, A. M. M. Eggermont, D. Haemmerich, G. A. Koning, *J. Controlled Release* **2013**, *167*, 130.
[72] B. B. Azad, S. R. Banerjee, M. Pullambhatla, S. Lacerda, C. A. Foss, Y. Wang, R. Ivkov, M. G. Pomper, *Nanoscale* **2015**, *7*, 4432.
[73] X. Ge, Q. Fu, L. Bai, B. Chen, R. Wang, S. Gao, J. Song, *New J. Chem.* **2019**, *43*, 8835.
[74] E. Gournaris, W. Park, S. Cho, D. J. Bentrem, A. C. Larson, D.-H. Kim, *ACS Appl. Mater. Interfaces* **2019**, *11*, 24.
[75] B. Li, L. Lu, M. Zhao, Z. Lei, F. Zhang, *Angew. Chem., Int. Ed.* **2018**, *57*, 7483.
[76] G. Deng, S. Li, Z. Sun, W. Li, L. Zhou, J. Zhang, P. Gong, L. Cai, *Theranostics* **2018**, *8*, 4116.
[77] a) Q. Li, J. Tan, B.-X. Peng, *Molecules* **1997**, *2*, 91; b) L. Zhang, D. Wang, K. Yang, D. Sheng, B. Tan, Z. Wang, H. Ran, H. Yi, Y. Zhong, H. Lin, Y. Chen, *Adv. Sci. (Weinheim, Ger.)* **2018**, *5*, 1800049.
[78] K. Mitra, C. E. Lyons, M. C. Hartman, *Angew. Chem., Int. Ed.* **2018**, *57*, 10263.
[79] W. Zou, C. Visser, J. A. Maduro, M. S. Pshenichnikov, J. C. Hummelen, *Nat. Photonics* **2012**, *6*, 560.
[80] S. Luo, X. Tan, Q. Qi, Q. Guo, X. Ran, L. Zhang, E. Zhang, Y. Liang, L. Weng, H. Zheng, *Biomaterials* **2013**, *34*, 2244.
[81] M. J. Duffy, O. Planas, A. Faust, T. Vogl, S. Hermann, M. Schäfers, S. Nonell, C. A. Strassert, *Photoacoustics* **2018**, *9*, 49.
[82] Y. Zhang, L. He, J. Wu, K. Wang, J. Wang, W. Dai, A. Yuan, J. Wu, Y. Hu, *Biomaterials* **2016**, *107*, 23.
[83] X. Li, X. Wang, C. Zhao, L. Shao, J. Lu, Y. Tong, L. Chen, X. Cui, H. Sun, J. Liu, *J. Nanobiotechnol.* **2019**, *17*, 23.
[84] S. Li, S. Zhou, Y. Li, X. Li, J. Zhu, L. Fan, S. Yang, *ACS Appl. Mater. Interfaces* **2017**, *9*, 22332.
[85] H. Li, X. Yang, Z. Zhou, K. Wang, C. Li, H. Qiao, D. Oupicky, M. Sun, *J. Controlled Release* **2017**, *261*, 126.
[86] H. Li, K. Wang, X. Yang, Y. Zhou, Q. Ping, D. Oupicky, M. Sun, *Acta Biomater.* **2017**, *53*, 399.
[87] Y. Shen, W. Lv, H. Yang, W. Cai, P. Zhao, L. Zhang, J. Zhang, L. Yuan, Y. Duan, *Cancer Lett. (N. Y., NY, U. S.)* **2019**, *455*, 14.
[88] Y. Deng, F. Käfer, T. Chen, Q. Jin, J. Ji, S. Agarwal, *Small* **2018**, *14*, 1802420.
[89] S. Ma, J. Zhou, Y. Zhang, B. Yang, Y. He, C. Tian, X. Xu, Z. Gu, *ACS Appl. Mater. Interfaces* **2019**, *11*, 7731.
[90] S.-Y. Lin, R.-Y. Huang, W.-C. Liao, C.-C. Chuang, C.-W. Chang, *Nanotheranostics* **2018**, *2*, 106.
[91] H. Lian, J. Wu, Y. Hu, H. Guo, *Int. J. Nanomed.* **2017**, *12*, 7777.
[92] F. Guo, M. Yu, J. Wang, F. Tan, N. Li, *ACS Appl. Mater. Interfaces* **2015**, *7*, 20556.
[93] Y. Xing, T. Ding, Z. Wang, L. Wang, H. Guan, J. Tang, D. Mo, J. Zhang, *ACS Appl. Mater. Interfaces* **2019**, *11*, 13945.
[94] X. Qiu, L. Xu, Y. Zhang, A. Yuan, K. Wang, X. Zhao, J. Wu, H. Guo, Y. Hu, *Mol. Pharmaceutics* **2016**, *13*, 829.
[95] J. Tian, B. Huang, H. Li, H. Cao, W. Zhang, *Biomacromolecules* **2019**, *20*, 6.
[96] W. He, Y. Jiang, Q. Li, D. Zhang, Z. Li, Y. Luan, *Acta Biomater.* **2019**, *84*, 356.
[97] K. Wang, Y. Zhang, J. Wang, A. Yuan, M. Sun, J. Wu, Y. Hu, *Sci. Rep.* **2016**, *6*, 27421.
[98] C. Zhao, Y. Tong, X. Li, L. Shao, L. Chen, J. Lu, X. Deng, X. Wang, Y. Wu, *Small* **2018**, *14*, 1703045.
[99] N. Li, F. Xu, J. Cheng, Y. Zhang, G. Huang, J. Zhu, X. Shen, D. He, *J. Biomed. Nanotechnol.* **2018**, *14*, 2162.
[100] Y. Xu, H. Ren, J. Liu, Y. Wang, Z. Meng, Z. He, W. Miao, G. Chen, X. Li, *Nanoscale* **2019**, *11*, 5474.
[101] H. Li, H. Liu, T. Nie, Y. Chen, Z. Wang, H. Huang, L. Liu, Y. Chen, *Biomaterials* **2018**, *178*, 620.
[102] Y. Tan, Y. Zhu, L. Wen, X. Yang, X. Liu, T. Meng, S. Dai, Y. Ping, H. Yuan, F. Hu, *Theranostics* **2019**, *9*, 691.
[103] A. Yuan, W. Huan, X. Liu, Z. Zhang, Y. Zhang, J. Wu, Y. Hu, *Mol. Pharmaceutics* **2016**, *14*, 242.
[104] G. Chen, K. Wang, Y. Zhou, L. Ding, A. Ullah, Q. Hu, M. Sun, D. Oupický, *ACS Appl. Mater. Interfaces* **2016**, *8*, 25087.
[105] K. Wang, G. Chen, Q. Hu, Y. Zhen, H. Li, J. Chen, B. Di, Y. Hu, M. Sun, D. Oupický, *Nanomedicine* **2017**, *12*, 1043.
[106] J. Song, L. Zhang, H. Yi, J. Huang, N. Zhang, Y. Zhong, L. Hao, K. Yang, Z. Wang, D. Wang, *Nanomedicine (N. Y., NY, U. S.)* **2019**, *20*, 102020.
[107] A. Samykutty, W. E. Grizzle, B. L. Fouts, M. W. McNally, P. Chuong, A. Thomas, A. Chiba, D. Otali, A. Woloszynska, N. Said, *Biomaterials* **2018**, *182*, 114.
[108] S. Li, J. Johnson, A. Peck, Q. Xie, *J. Transl. Med.* **2017**, *15*, 18.
[109] H. Han, J. Wang, T. Chen, L. Yin, Q. Jin, J. Ji, *J. Colloid Interface Sci.* **2017**, *507*, 217.
[110] A. Ullah, K. Wang, P. Wu, D. Oupicky, M. Sun, *Int. J. Nanomed.* **2019**, *14*, 2927.
[111] Y. Lee, S. Lee, S. Jon, *Adv. Sci. (Weinheim, Ger.)* **2018**, *5*, 1800017.
[112] Y. Han, Z. Chen, H. Zhao, Z. Zha, W. Ke, Y. Wang, Z. Ge, *J. Controlled Release* **2018**, *284*, 15.
[113] H. Luo, Q. Wang, Y. Deng, T. Yang, H. Ke, H. Yang, H. He, Z. Guo, D. Yu, H. Wu, *Adv. Funct. Mater.* **2017**, *27*, 1702834.
[114] M. Guo, J. Huang, Y. Deng, H. Shen, Y. Ma, M. Zhang, A. Zhu, Y. Li, H. Hui, Y. Wang, *Adv. Funct. Mater.* **2015**, *25*, 59.
[115] M. Guo, H. Mao, Y. Li, A. Zhu, H. He, H. Yang, Y. Wang, X. Tian, C. Ge, Q. Peng, *Biomaterials* **2014**, *35*, 4656.
[116] Y. Deng, L. Huang, H. Yang, H. Ke, H. He, Z. Guo, T. Yang, A. Zhu, H. Wu, H. Chen, *Small* **2017**, *13*, 1602747.

[117] H. Yang, H. Mao, Z. Wan, A. Zhu, M. Guo, Y. Li, X. Li, J. Wan, X. Yang, X. Shuai, *Biomaterials* **2013**, *34*, 9124.
[118] C.-S. Yeh, C.-H. Su, W.-Y. Ho, C.-C. Huang, J.-C. Chang, Y.-H. Chien, S.-T. Hung, M.-C. Liau, H.-Y. Ho, *Biomaterials* **2013**, *34*, 5677.
[119] R. G. Thomas, M. J. Moon, S. P. Surendran, H. J. Park, I.-K. Park, B.-I. Lee, Y. Y. Jeong, *Mol. Imaging Biol.* **2018**, *20*, 533.
[120] S. Lee, R. George Thomas, M. Ju Moon, H. Ju Park, I.-K. Park, B.-I. Lee, Y. Yeon Jeong, *Sci. Rep.* **2017**, *7*, 2108.
[121] R. P. Johnson, Y. I. Jeong, J. V. John, C. W. Chung, S. H. Choi, S. Y. Song, D. H. Kang, H. Suh, I. Kim, *Macromol. Rapid Commun.* **2014**, *35*, 888.
[122] H. Han, H. Wang, Y. Chen, Z. Li, Y. Wang, Q. Jin, J. Ji, *Nanoscale* **2016**, *8*, 283.
[123] L. Shao, Q. Li, C. Zhao, J. Lu, X. Li, L. Chen, X. Deng, G. Ge, Y. Wu, *Biomaterials* **2019**, *194*, 105.
[124] X. Song, R. Zhang, C. Liang, Q. Chen, H. Gong, Z. Liu, *Biomaterials* **2015**, *57*, 84.
[125] X. Liang, L. Fang, X. Li, X. Zhang, F. Wang, *Biomaterials* **2017**, *132*, 72.
[126] Z. Yang, J. Song, W. Tang, W. Fan, Y. Dai, Z. Shen, L. Lin, S. Cheng, Y. Liu, G. Niu, *Theranostics* **2019**, *9*, 526.
[127] S. H. Kim, J. E. Lee, S. M. Sharker, J. H. Jeong, I. In, S. Y. Park, *Biomacromolecules* **2015**, *16*, 3519.
[128] L. Meng, S. Gan, Y. Zhou, Y. Cheng, Y. Ding, X. Tong, J. Wu, Y. Hu, A. Yuan, *Biomater. Sci.* **2019**, *7*, 168.
[129] L. Meng, Y. Cheng, S. Gan, Z. Zhang, X. Tong, L. Xu, X. Jiang, Y. Zhu, J. Wu, A. Yuan, *Mol. Pharmaceutics* **2018**, *15*, 447.
[130] Y. Zhao, G. Chen, Z. Meng, G. Gong, W. Zhao, K. Wang, T. Liu, *Drug Delivery* **2019**, *26*, 717.
[131] Y. Li, Y. Du, X. Liu, Q. Zhang, L. Jing, X. Liang, C. Chi, Z. Dai, J. Tian, *Mol. Imaging* **2015**, *14*, 7.
[132] L. Jing, S. Shao, Y. Wang, Y. Yang, X. Yue, Z. Dai, *Theranostics* **2016**, *6*, 1.
[133] M.-M. Chen, Y.-Y. Liu, G.-H. Su, F.-F. Song, Y. Liu, Q.-Q. Zhang, *Int. J. Nanomed.* **2017**, *12*, 4225.
[134] Y. Wang, Z. Sun, Z. Chen, Y. Wu, Y. Gu, S. Lin, Y. Wang, *Anal. Chem.* **2019**, *91*, 3.
[135] L. Sha, Q. Zhao, D. Wang, X. Li, X. Wang, X. Guan, S. Wang, *J. Colloid Interface Sci.* **2019**, *535*, 380.
[136] T. H. Tran, H. T. Nguyen, N. Van Le, T. T. P. Tran, J. S. Lee, S. K. Ku, H.-G. Choi, C. S. Yong, J. O. Kim, *Int. J. Pharm. (Amsterdam, Neth.)* **2017**, *528*, 692.
[137] R. K. Thapa, H. T. Nguyen, M. Gautam, A. Shrestha, E. S. Lee, S. K. Ku, H.-G. Choi, C. S. Yong, J. O. Kim, *Drug Delivery* **2017**, *24*, 1690.
[138] B. Wu, B. Wan, S.-T. Lu, K. Deng, X.-Q. Li, B.-L. Wu, Y.-S. Li, R.-F. Liao, S.-W. Huang, H.-B. Xu, *Int. J. Nanomed.* **2017**, *12*, 4467.
[139] T. Li, X. Shen, X. Xie, Z. Chen, S. Li, X. Qin, H. Yang, C. Wu, Y. Liu, *Nanomedicine* **2018**, *13*, 595.
[140] C. Wu, L. Wang, Y. Tian, X. Guan, Q. Liu, S. Li, X. Qin, H. Yang, Y. Liu, *ACS Appl. Mater. Interfaces* **2018**, *10*, 6942.
[141] Q. Chen, C. Wang, Z. Zhan, W. He, Z. Cheng, Y. Li, Z. Liu, *Biomaterials* **2014**, *35*, 8206.
[142] Y. Yang, J. Liu, C. Liang, L. Feng, T. Fu, Z. Dong, Y. Chao, Y. Li, G. Lu, M. Chen, *ACS Nano* **2016**, *10*, 2774.
[143] E. B. Kang, J. E. Lee, Z. A. I. Mazrad, I. In, J. H. Jeong, S. Y. Park, *Nanoscale* **2018**, *10*, 2512.
[144] C. A. Choi, J. E. Lee, Z. A. I. Mazrad, Y. K. Kim, I. In, J. H. Jeong, S. Y. Park, *ChemMedChem* **2018**, *13*, 1459.
[145] Y. Zhang, D. Yang, H. Chen, W. Q. Lim, F. S. Z. Phua, G. An, P. Yang, Y. Zhao, *Biomaterials* **2018**, *163*, 14.
[146] Q. Chen, C. Wang, L. Cheng, W. He, Z. Cheng, Z. Liu, *Biomaterials* **2014**, *35*, 2915.
[147] Y. Chang, X. Li, X. Kong, Y. Li, X. Liu, Y. Zhang, L. Tu, B. Xue, F. Wu, D. Cao, *J. Mater. Chem. B* **2015**, *3*, 8321.